Lehigh University
Lehigh Preserve

Fritz Laboratory Reports | Civil and Environmental Engineering

1958

Rotation capacity requirements for single-span frames, Lehigh University, (1958)

G. C. Driscoll Jr.

Follow this and additional works at: http://preserve.lehigh.edu/engr-civil-environmental-fritz-lab-reports

Recommended Citation
Driscoll, G. C. Jr., "Rotation capacity requirements for single-span frames, Lehigh University, (1958)" (1958). *Fritz Laboratory Reports.* Paper 79.
http://preserve.lehigh.edu/engr-civil-environmental-fritz-lab-reports/79

This Technical Report is brought to you for free and open access by the Civil and Environmental Engineering at Lehigh Preserve. It has been accepted for inclusion in Fritz Laboratory Reports by an authorized administrator of Lehigh Preserve. For more information, please contact preserve@lehigh.edu.

Welded Continuous Frames and Their Components

Progress Report No. 31

ROTATION CAPACITY REQUIREMENTS FOR SINGLE-SPAN FRAMES

by

George C. Driscoll, Jr.

FRITZ ENGINEERING
LABORATORY LIBRARY

This work has been carried out as a part of an investigation sponsored jointly by the Welding Research Council and the Department of the Navy with funds furnished by the following:

American Institute of Steel Construction
American Iron and Steel Institute
Institute of Research, Lehigh University
Office of Naval Research (Contract Nonr 61003)
Bureau of Ships
Bureau of Yards and Docks

Reproduction of this report in whole or in part is permitted for any purpose of the United States Government.

Fritz Engineering Laboratory
Department of Civil Engineering
Lehigh University
Bethlehem, Pennsylvania
September, 1958
Fritz Laboratory Report No. 268.5

TABLE OF CONTENTS

ABSTRACT

Plastic analysis of steel structures depends on the ability of the members to form plastic hinges, and to redistribute moments. In order for redistribution of moment to take place, certain plastic hinges must sustain their plastic moment through some angle of rotation. The amount of rotation required may affect the stability of the structure and therefore, may affect the geometry of the structural shapes selected and the spacing of lateral bracing. The ability of a structural member to rotate in order to redistribute moments and form a mechanism is defined as the "rotation capacity". The angle of rotation during which a yielded segment of beam must sustain its plastic moment value is termed the "hinge angle".

An earlier report on continuous beams presented the equations and methods of handling the boundary conditions for the calculation of the required hinge angles of structures.[3] This paper extends that work to cover the calculation of required hinge angles for single-span portal frames with pinned bases.

1. INTRODUCTION

Recent developments in the plastic analysis of steel frames have presented a more rational basis on which to design welded continuous structures. Methods based on these developments give promise of economies to be gained by taking advantage of the reserve of strength of structural steel beyond the elastic limit, by using simple methods of analysis, and by assuring a uniform factor of safety against failure for all structures.[2]

Plastic analysis of steel structures depends on the ability of the members to form plastic hinges and to redistribute moments. In order for redistribution of moment to take place, certain plastic hinges must sustain their plastic moment through some angle of rotation. The amount of rotation required may affect the stability of the structure and, therefore, may affect the geometry of the structural shapes selected and the spacing of lateral bracing. The ability of a structural member to rotate at or near its plastic moment is defined as rotation capacity. The angle of rotation during which a yielded segment of beam must sustain its plastic moment value is termed the required "hinge angle".

This paper deals with the calculation of the approximate hinge angles required to allow mechanisms to form in single-span gabled portal frames with pinned bases. The development of the basic method of solution is presented in an earlier paper on three-span beams.[3] There, it is shown that calculations of rotation and deflection may be made by using modified slope-deflection equations with

appropriate boundary conditions. The dominant boundary condition is shown to be continuity at the last plastic hinge to form. The same basic method of solution will be used in this paper without resorting to complete development of the method.

Finally, an attempt will be made to determine the maximum required hinge angles for practical sizes and shapes of frames under the probable ranges of loading for which they might be designed.

2. DERIVATION OF HINGE ANGLE EQUATIONS

Prior to deriving equations for the required hinge angles, the proportions of the frames will be stated and the boundary conditions governing the solution of the problem will be determined.

Ketter[6] has presented equations and charts which permit the rapid design of single and multiple span frames. This work will be referred to in order to obtain the required plastic moment for the various possible mechanisms. The same system of notation will be followed closely in the development of hinge angle equations.

2.1 MECHANISMS, DOMAINS, AND PLASTIC MOMENT VALUES

Consider the typical gabled portal frame with pinned bases shown in Fig. 1. The frame has a span L, a column height of aL and a roof rise bL. The special case of a flat roofed frame is obtained when b equals zero. Rolled structural shapes of constant cross section are assumed. A uniformly distributed vertical load of w pounds per foot is applied to the entire roof. The effect of all horizontal forces is represented by a load P equal to AwL/2a applied at the top of the windward column.

The possible mechanisms which determine the maximum load of this frame are a sidesway or panel mechanism (Fig. 2a) and a general composite mechanism (Fig. 2b).

For the panel mechanism, the relationship between plastic moment and ultimate load is:[6]

$$\frac{M_p}{wL^2} = \frac{A}{4} \qquad \ldots(1)$$

The maximum load-moment expression for the composite mechanism is:[6]

$$\frac{M_p}{wL^2} = \frac{1}{4}\left[\frac{(1-\alpha)(A+\alpha)}{1+\frac{b}{a}\alpha}\right]$$

where

$$\alpha = \frac{1}{\frac{b}{a}}\left[\sqrt{1-\frac{b}{a}\left[A\left(1+\frac{b}{a}\right)-1\right]}-1\right] \qquad \text{for} \frac{b}{a} > 0$$

or

$$\alpha = \frac{1-A}{2} \qquad \text{for } \frac{b}{a} = 0 \qquad \ldots(2)$$

Equating these two expressions will give an expression defining values of b, a, and A for which both of the mechanisms will form simultaneously. The expression will also indicate the boundary between the regions where the two mechanisms predominate, or

$$A = \frac{1}{1+\frac{b}{a}} \qquad \ldots(3)$$

This equation is plotted as a family of curves in Fig. 3. A separate curve relating side load and column height is given for each value of the roof rise factor, b, from 0 to 1.0. If at a given column height, the side load factor A falls below the appropriate curve, the composite mechanism will form. For values of the side load factor above the curve, a panel mechanism will form.

2.2 LOCATION OF FIRST AND LAST PLASTIC HINGES

Since the structure under consideration is indeterminate to the first degree, two hinges will be sufficient to form a mechanism.

Determination of the location of the first plastic hinge by means of an elastic solution will then give the location of the last plastic hinge by elimination.

Plastic hinges are shown in Fig. 2 to exist only at the two knees, C and E, and in the windward rafter at F. An elastic solution will give the following values for the moments at these points.

Moment at Windward Knee

$$M_C = \frac{wL^2}{8} \left[A(F+J) \quad - \quad G \right] \qquad \ldots(4)$$

Moment at Lee Knee

$$M_E = - \frac{wL^2}{8} \left[AF + G \right] \qquad \ldots(5)$$

Maximum Moment in Windward Rafter

$$M_F = \frac{wL^2}{8} \left[1 + 2A + A^2 + \frac{b}{a} F(A^2 - A) \quad -AF + \frac{b}{a} GA \right.$$
$$\left. - \frac{b}{a} G - G + \frac{1}{4} \frac{b^2}{a^2} \quad (G + AF)^2 \right] \qquad \ldots(6)$$

In the above equations a plus (+) sign designates a moment which causes tension on the inside of the frame. The functions F, G, J, and N are given by:

$$F = \left[\frac{\sqrt{\frac{16a}{1+4b^2}} + \quad 24 + 12\frac{b}{a}}{N} \right]$$

$$G = \left[\frac{8 + 5\frac{b}{a}}{N}\right]$$

$$J = \left[24\,\frac{b}{a} + 16\,\frac{b^2}{a^2}\right]$$

$$N = \left[\frac{8a}{\sqrt{1+4b^2}} + 12 + 12\frac{b}{a} + 4\,\frac{b^2}{a^2}\right] \qquad \ldots(7)$$

Equations 4 through 7 are derived from superposition of two cases given in Ref. 5. The substitutions F, G, J, and N have been made to reduce the bulk of the equations, and the load parameter A has been added.

Because hinge E is common to both mechanisms, the problem of location of first plastic hinge reduces to finding when M_C and M_F equal M_E.

By equating M_C and $-M_E$ and making the substitutions in Eq. 7, the following boundary between first plastic hinge at E or at C is obtained:

$$A = \frac{8 + 5\frac{b}{a}}{12\frac{b}{a} + 8\frac{b^2}{a^2}} \qquad \text{for } b > 0 \qquad \ldots(8)$$

When b=0, the first hinge cannot occur at C.

Another limit on the first hinge at E is the occurrence of an equal or greater elastic moment at F. The boundary for this case is obtained by equating M_F and $-M_E$.

$$0 = A^2 \left(1+\frac{b}{a} F + \frac{1}{4} \frac{b^2}{a^2} F^2\right) + A \left(2 - \frac{b}{a} F - 2F + \frac{b}{a} G + \frac{1}{2} \frac{b^2}{a^2} FG\right)$$

$$+ \left(1-\frac{b}{a} G - 2G + \frac{1}{4} \frac{b^2}{a^2} G^2\right) \qquad \text{for } b > 0 \qquad \ldots(9)$$

$$A = 1 - 2\sqrt{\frac{1}{2a+3}} \qquad \text{for } b = 0$$

Equation (8) is plotted as a family of solid curves passing through the origin in Fig. 4. The region above the curve for a given value of the roof rise factor b, represents the values of A and a for which the first plastic hinge will form at the windward knee C. Below the curve, the first hinge will form at the lee knee E.

Equations (9) and (10) are also plotted in Fig. 4, as a family of dashed curves. These curves divide the values of A and a for which the first plastic hinge will form at a point F in the windward rafter, from the values for which the first hinge will form at the lee knee, E. It will be noted that the first hinge can form in the rafter only for small values of b, the largest being about 0.387, when the column height is no greater than the frame span.

Figs. 5 and 6 are charts showing the limits of mechanisms for b values of 0, and 0.2 respectively. On these charts, a shaded area above the line representing Eq. (3) denotes the frame sizes and loading for which a panel mechanism will occur, while the clear area, indicates the general composite mechanism. An additional line in the shaded area representing Eq. (8) separates

the regions in which the first plastic hinge will form at the windward knee C or in the lee knee E. A final line in the unshaded area separates the region in which the first hinge forms at E from the region in which the first plastic hinge forms in the rafter at F. This curve represents Eq. (9) or (10) as applicable.

It may be seen from Fig. 5 that a panel or sidwsway mechanism will not occur in a flat-roofed frame with the proportions and loading considered in this study. From Eq. (3) it will be seen that the panel mechanism could occur when A exceeds 1.0.

2.3 HINGE ANGLE EQUATIONS

Derivation of equations for hinge angles of single span portal frames is accomplished through the use of the slope-deflection equation:[3]

$$\theta_{NF} = \theta'_{NF} + R_{NF} + \frac{\ell}{3EI}\left(M_{NF} - \frac{1}{2} M_{FN}\right) \qquad \ldots(11)$$

θ_{NF} = Slope of near end of member

θ'_{NF} = Slope of near end of similarly loaded member when simply supported

R_{NF} = Rotation of a chord between ends of member

= Deflection of one end of a member with respect to the other divided by the distance between them = Δ/ℓ

ℓ = Length of member or portion of member

M_{NF} = Moment at near end of member

M_{FN} = Moment at far end of member

For cases with sloping roofs, the θ' term is expressed in a manner which takes into account the slant of the roof. For symmetrical

gabled roofs where the dimensions are measured as shown in Fig. 1 the expression is:

$$\theta' = \frac{w\ell H^3}{24EI} \sqrt{1+4b^2} \qquad \ldots(12)$$

where $\ell_{(i)}$ = the horizontal projection of the length of a segment.

The sign convention used here is that slope angles are defined as positive when the rotations are clockwise, and end moments are defined as positive when acting in the clockwise sense. (see Fig. 8).

θ with appropriate subscript is used to represent the slope on both sides of a hinge location. H, the hinge angle, is used to represent the difference in slope at a plastic hinge when the maximum load is first reached.

The ultimate load moment diagram for the frame is shown in Fig. 7a with the effect of each type of force kept separated.

Case I. Composite Mechanism--First Hinge at Lee Knee E

The first solution will be that for the general composite type of mechanism with the first plastic hinge at the lee column top (E). The boundary conditions for this solution are the continuity at joints C and D. At joint E, the slope will be discontinuous. Substituting the moment values from Fig. 7a, in Eq. (11), will form two slope equations for each member. Since there is no transverse load on the columns, the θ' terms for those members do not exist. Pertinent lengths for use in the slope-deflection equations are given in Fig. 7b.

The end slope equations for each member as as follows:

Member AC

$$\theta_A = R_{AC} + \frac{aL}{3EI}\left[\ 0-\frac{1}{2}\left(\ -\frac{AwL^2}{2} + M_p\right)\right]$$

$$\theta_C = R_{AC} + \frac{aL}{3EI}\left[\left(-\frac{AwL^2}{2} + M_p\right) \ - 0\right]$$

Member CD

$$\theta_C = \frac{wL^3}{192EI}\sqrt{1+4b^2} + R_{CD} + L\sqrt{\frac{1+4b^2}{6EI}}\left\{\frac{AwL^2}{2} - M_p - \frac{1}{2}\left[M_p\left(1+\frac{b}{a}\right) - \frac{wL^2}{8} - \frac{AwL^2}{4}\right]\right\}$$

$$\theta_D = \frac{-wL^3}{192EI}\sqrt{1+4b^2} + R_{CD} + L\sqrt{\frac{1+4b^2}{6EI}}\left\{M_p\left(1+\frac{b}{a}\right) - \frac{wL^2}{8} - \frac{wL^2}{4} - \frac{1}{2}\left[\frac{AwL^2}{2} - M_p\right]\right\}$$

Member DE

$$\theta_D = \frac{wL^3}{192EI}\sqrt{1+4b^2} + R_{DE} + L\sqrt{\frac{1+4b^2}{6EI}}\left\{-M_p\left(1+\frac{b}{a}\right) + \frac{wL^2}{8} + \frac{AwL^2}{4} - \frac{1}{2}\left[M_p\right]\right\}$$

$$\theta_{ED} = \frac{wL^3}{192EI}\sqrt{1+4b^2} + R_{DE} + L\sqrt{\frac{1+4b^2}{6EI}}\left\{M_p - \frac{1}{2}\left[M_p\ \left(1+\frac{b}{a}\right) + \frac{wL^2}{8} + \frac{AwL^2}{4}\right]\right\}$$

Member EB

$$\theta_{EB} = R_{BE} + \frac{aL}{3EI}\left[-M_p - 0\right]$$

$$\theta_B = R_{BE} + \frac{aL}{3EI}\left[0 - \frac{1}{2}\ (-M_p)\right] \qquad \ldots(13)$$

These eight equations have six unknown θ's and four unknown R's. The two additional equations necessary for the solution of the problem may be obtained by considering the relative vertical and horizontal displacements of the pinned bases. These are the equations generally used to take sidesway into account in slope-deflection solutions of structures. The relative vertical displacement of the bases

is zero and is obtained by multiplying the chord rotation R of each member by the horizontal component of its length and summing these for the structure.

$$R_{CD}\frac{L}{2} + R_{DE}\frac{L}{2} = 0 \qquad \ldots(14)$$

The relative horizontal displacement of the bases is obtained by summing the products of the chord rotations R and the vertical components of the length of each member. Since positive rotations of members DE and EB cause negative displacements of the base B, the signs of these terms change.

$$R_{AC}\,aL + R_{CD}\,bL - R_{DE}\,bL - R_{BE}\,aL = 0 \qquad \ldots(15)$$

Solution of the Equations (13), (14), and (15) for θ_{ED} and θ_{EB} gives the following:

$$\theta_{ED} = L\sqrt{\frac{1+4b^2}{6EI}}\left[M_p\left(3+\frac{3}{2}\frac{b}{a}\right) - \frac{1}{4}wL^2 - \frac{1}{2}AwL^2\right] \qquad \ldots(16)$$

$$\theta_{EB} = L\sqrt{\frac{1+4b^2}{6EI}}\left[M_p\left(-3-\frac{9}{2}\frac{b}{a} - \frac{2b^2}{a^2}\right) + wL^2\left(\frac{1}{4} + \frac{5}{16}\frac{b}{a}\right) + AwL^2\left(1+\frac{3}{4}\frac{b}{a}\right)\right]$$

$$- \frac{2}{3}\frac{M_{pL}a}{EI} + \frac{1}{6}\frac{AwL^2a}{EI} \qquad \ldots(17)$$

The hinge angle at E is equal to the difference in θ_{EB} and θ_{ED}.

$$H_E = L\sqrt{\frac{1+4b^2}{EI}}\left[M_p\left(-1-\frac{b}{a} - \frac{1}{3}\frac{b^2}{a^2}\right) + wL^2\left(\frac{1}{12} + \frac{5}{96}\frac{b}{a}\right) + AwL^2\left(\frac{1}{4} + \frac{1b}{8a}\right)\right]$$

$$- \frac{2}{3}\frac{M_{pL}}{EI}a + \frac{1}{6}\frac{AwL^2}{EI}a \qquad \ldots(18)$$

In non-dimensional form, this equation is:

$$\frac{H_E}{\phi_p L} = \sqrt{1+4b^2}\left\{\frac{wL^2}{M_p}\left[\frac{1}{12}+\frac{5}{96}\frac{b}{a}+A\left(\frac{1}{4}+\frac{1}{8}\frac{b}{a}\right)\right]-\left[1+\frac{b}{a}+\frac{1}{3}\frac{b^2}{a^2}\right]\right\}$$

$$-\frac{2}{3}a+\frac{1}{6}a\frac{wL^2}{M_p}A \qquad \ldots(19)$$

where

$$\phi_p = \frac{M_p}{EI} \qquad \ldots(20)$$

(curvature ϕ_p is that curvature for which the moment just reaches M_p).

For a flat roofed frame, the equation reduces to:

$$\frac{H_E}{\phi_p L} = \frac{wL^2}{M_p}\left[\frac{1}{12}+A\left(\frac{1}{4}+\frac{1}{6}a\right)\right]-1-\frac{2}{3}a \qquad \ldots(21)$$

Values of M_p/wL^2 may be obtained from Eq. (2) or reference 6 thus making it possible to plot curves of hinge angles as shown in Figs. 9 and 10. Eqs. (19) and (21) give the hinge angles for all cases in which the values of a, b, and A fall within the domain indicating formation of a general composite mechanism with first hinge at E in Figs. 3, 4, 5, and 6.

Case II. Composite Mechanism--First Hinge in Windward Rafter at F

As was shown in Section 2.2, for certain proportions of the frame and for certain loadings the first plastic hinge will form in the rafter. In this case, the discontinuity occurs at point F in the rafter, and elastic continuity is maintained up to ultimate load at the lee knee, E. The ultimate load moment diagram is again as shown in Fig. 7a.

In setting up the slope-deflection equations for this case, it is necessary to write two equations for each of the segments CF and FD of member CD. Besides the slope-deflection equations, two additional equations are again derived from considering the horizontal and vertical components of the movement of base B equal to zero. For the vertical displacement, this equation is:

$$R_{CF}\,\alpha\,L + R_{FD}\left(\frac{1}{2} - \alpha\right)L + R_{DE}\,\frac{L}{2} = 0 \qquad \ldots(22)$$

For the horizontal displacement the equation is:

$$R_{AC}\,aL + R_{CF}2b\,\alpha L + R_{FD}\,(bL-2b\alpha L) - R_{DE}bL - R_{BE}aL = 0 \qquad \ldots(23)$$

Solution in the same manner as for the previous case results in the following equation for the hinge angle, H_F:

$$\frac{H_F}{\phi_p L} = \frac{1}{(1+2\frac{b}{a}\alpha)}\left\{\frac{1}{6}\,a\,\frac{wL^2}{M_p}\,A - \frac{2}{3}\,a + \sqrt{1+4b^2}\left\{\frac{wL^2}{M_p}\left[\frac{1}{12} + \frac{5}{96}\,\frac{b}{a} + A\left(\frac{1}{4} + \frac{1}{8}\,\frac{b}{a}\right)\right] - \left[1 + \frac{b}{a} + \frac{1}{3}\,\frac{b^2}{a^2}\right]\right\}\right\} \qquad \ldots(24)$$

Note that the second factor of the product in Eq. (24) is equal in magnitude to Eq. (19). When Eq. (19) and (24) are both zero, H_E equals H_F, and both plastic hinges form simultaneously, with zero hinge angle required.

For flat roofed frames,

$$\frac{H_F}{\phi_p L} = \frac{wL^2}{M_p}\left[\frac{1}{12} + A\left(\frac{1}{4} + \frac{1}{6}a\right)\right] - 1 - \frac{2}{3}\,a \qquad \ldots(25)$$

In Eq. (24), α is the parameter giving the horizontal distance αL from joint C to the plastic hinge F in the rafter. Values of α may be obtained from Reference 6 or the equation,

$$\alpha = \frac{1}{\frac{b}{a}}\left[\sqrt{1 + \frac{b}{a}\left[A\left(1+\frac{b}{a}\right) - 1\right]} - 1\right] \qquad \ldots(26)$$

Equations (24) and (25) give the hinge angles only for those cases in which a, b, and A fall in the domain indicated in the appropriate Figs. 3 to 6.

Case Ia. Panel Mechanism--First Hinge at Lee Knee E

For cases where the loading and dimensions are such as to make the value of α equal to zero, the rafter hinge occurs at the windward knee and a panel mechanism results. In the usual panel mechanism, the first hinge occurs at the lee knee, E, and it is there that the hinge angle is required.

The ultimate load moment diagram for the panel mechanism is the same as for the composite mechanism (Fig. 7a) with the special requirements that α equal zero and Eq. (1) hold for M_p/wL^2. Therefore, making these substitutions in Eq. (19), the resulting expression for the hinge angle is:

$$\frac{H_E}{\phi_p L} = \sqrt{1+4b^2}\left[\frac{1}{A}\left(\frac{1}{3} + \frac{5}{24}\frac{b}{a}\right) - \left(\frac{1}{2}\frac{b}{a} + \frac{1}{3}\frac{b^2}{a^2}\right)\right] \qquad \ldots(27)$$

For flat roofed frames, Eq. (21) reduces to:

$$\frac{H_E}{\phi_p L} = \frac{1}{3A} \qquad \ldots(28)$$

Eqs. (27) and (28) give the hinge angle at the lee knee, E, for a panel mechanism when a, b, and A fall within the proper domain of Figs. 3 to 6.

Case IIa. Panel Mechanism--First Hinge at Windward Knee C

Certain gabled frames as shown in the domain Figs. 4 and 6 may form a panel mechanism with the first plastic hinge at the windward knee C. This is a special condition on Case II where the value of α equals zero so that point F is at point C. All results of Case II at point F become equal to the corresponding results for point C when α is set equal to zero and Eq. (1) is substitutued for M_p/wL^2. The hinge angle at joint C then becomes:

$$\frac{H_C}{\emptyset_p L} = \sqrt{1+4b^2}\left[\frac{1}{A}\left(\frac{1}{3}+\frac{5}{24}\frac{b}{a}\right) - \left(\frac{1}{2}\frac{b}{a}+\frac{1}{3}\frac{b^2}{a^2}\right)\right] \quad \ldots(29)$$

For flat roofed frames, it is impossible for the first plastic hinge to occur at joint C as shown by Eq. (8).

Though Eq. (29) is identical to Eq. (27), it must be borne in mind that they usually apply to different values of a, b and A, and thus the values of H_C and H_E will coincide only when Eq. (8) is satisfied.

2.4 DESCRIPTION OF GRAPHS OF HINGE ANGLE EQUATIONS

Graphs of the hinge angle function are plotted for two values of the roof rise factor b. Figure 9 presents the hinge angles for frames with flat roofs (b=0), and Fig. 10 the hinge angles for gabled

frames with roof rise factor b = 0.2. Each of the graphs shows the non-dimensional magnitude of the hinge angle ($H/\emptyset_p L$) plotted versus the column height factor, a. These hinge angle curves are plotted for values of the side load factor A ranging from 0 to 1.0. The line for A = 0 is hatched, indicating the initial value of the function. Initially, only values of H on and above this line are valid. With increasing side load, the sloping lines indicating the hinge angles for larger values of A gradually move upward and decrease in slope. When the value of A reaches about 0.5 for flat roofs and 0.3 for b = 0.3, the hinge angle function begins to decrease with increasing values of side load factor A.

With the aid of small sketches of the mechanisms on each graph, the controlling plastic hinge and equation may be identified. The major portion of each graph is that part above the abscissa which gives values of the hinge angle, H_E, at the lee knee representing Eq. (19) and (21) for the composite mechanism. A small sketch of the composite mechanism adjacent to that area indicates that the first hinge forms at the lee knee and the second hinge in the windward portion of the roof member. Comparable sketches identify the portions of the graph comprising the other cases. Additional values of H_E occur with a panel mechanism which occurs at high side loads. For flat roofed frames the panel mechanism is denoted by A = 1.0 and greater (Eq. 28). For gabled frames, results of Eq. (27) appear below the dashed line in Fig. 10 and above the abscissa.

For the gabled frames in Fig. 11 the hinge angle curves for A = 0.5 to 1.0 drop below the abscissa at the left side of the graph.

These are the result of Eq. (29) for the hinge angle, H_C, at the windward knee in a panel mechanism.

One more area of importance appears in each graph. This is the area bounded by the A = 0 line below the abscissa. In this region, with very light side loads and longer columns, the first hinge forms in the windward rafter at F with a composite mechanism resulting. The values of H_F are calculated from Eq. (24) and (25). Many practical cases may be covered by this region because of the absence of side load.

2.5 DERIVATION OF EQUATIONS FOR DEFLECTIONS

From the same solution which results in the equations for hinge angles, the horizontal deflections of the knees and the vertical deflection of the ridge may be derived.

Case I. Composite Mechanism--First Hinge at Lee Knee E

Simultaneous equations (13), (14) and (15) may be solved for the chord rotations R_{AC}, R_{DE}, and R_{BE}. Then, since the horizontal deflection, δ_E, of the lee knee equals $R_{BE}\, aL$,

$$\frac{\delta_E}{\phi_p L^2} = a\sqrt{1+4b^2}\left\{\frac{wL^2}{M_p}\left[\frac{1}{24}+\frac{5}{96}\frac{b}{a}+A\left(\frac{1}{6}+\frac{1}{8}\frac{b}{a}\right)\right]-\left[\frac{1}{2}+\frac{3}{4}\frac{b}{a}+\frac{1}{3}\frac{b^2}{a^2}\right]\right\}$$

$$\frac{1}{3}a^2+\frac{1}{6}a^2\,\frac{wL^2}{M_p}\,A \qquad \ldots(30)$$

In the same manner, R_{AC} may be used to obtain the value of δ_C, the horizontal deflection of the windward knee.

$$\frac{\delta_C}{\phi_p L^2} = a\sqrt{1+4b^2}\left[\frac{wL^2}{M_p}\left(\frac{1}{24}+\frac{1}{6}A\right) - \left(\frac{1}{2}+\frac{1}{4}\frac{b}{a}\right)\right] - \frac{1}{3}a^2 + \frac{1}{6}a^2\frac{wL^2}{M_p}A \quad \ldots(31)$$

Since the vertical deflection, δ_D, of the ridge equals $-R_{DE}\,L/2$,

$$\frac{\delta_D}{\phi_p L^2} = \sqrt{1+4b^2}\left[\frac{wL^2}{M_p}\left(\frac{5}{384}+\frac{1}{32}A\right) - \left(\frac{1}{8}+\frac{1}{12}\frac{b}{a}\right)\right] \quad \ldots(32)$$

Similar methods give equations for deflections for all the cases. These are summarized in the appendix of reference 2.

Graphs of deflections are plotted in Figs. 11 through 15. In each graph, a deflection function δ is plotted against column height factor, a, for a number of side load factors, A.

Figs. 11 and 12, give the horizontal deflection of the knees and the vertical deflection of the middle of the beam for flat-roofed frames. Figs. 13 and 14 give the horizontal deflections of the two knees of gabled frames ($b = 0.2$), while Fig. 15 gives the vertical deflection of the ridges of gabled frames.

The style of the deflection graphs is the same as that of the hinge angle graphs described in Section 24. There should be no particular difficulty in reading the graphs.

3. ILLUSTRATIVE EXAMPLE--GABLED FRAME

The equations derived here make it possible to determine the hinge angles required to form a mechanism as well as the deflections of joints of a large variety of portal frames. The equations will serve for all symmetrical frames with pinned bases as long as the loads may be approximated by uniformly distributed vertical loads. The effect of horizontal loads is replaced by a concentrated horizontal load at the eaves of such magnitude as to cause the same moment about the base. Use of the results of this study will be illustrated by an example of a gabled frame which will be compared with experimental results.

Given: Span length, $L = 40$ ft.

Column height, $aL = 10$ ft.

Roof rise $bL = 8$ ft.

Bent spacing $s = 17$ ft.

Vertical working loads:

Dead plus live, plus snow 60 psf.

Horizontal working load:

Wind, 20 psf

Load factors:

Dead plus live load, 1.88
Dead plus live plus wind load 1.41
σ_y, 33 ksi
E, 30,000 ksi

Find: Rolled structural shape for the frame.

Hinge angle required to form a mechanism.

Deflections at maximum load.

a. Design

From the given data, the parameters for geometry of the frame are found to be:

$$a = 0.25$$

$$b = 0.20$$

$$b/a = 0.8$$

The vertical design load for dead load plus live load for the 17 ft. bent spacing and 60 psf working load is:

$$w = 60 \text{ psf} \times 17 \text{ ft.} \times 1.88 = 1918 \text{ lb./ft.}$$

Using the load factor for dead plus live plus wind load, the design load becomes:

$$w = 60 \text{ psf} \times 17 \text{ ft.} \times 1.41 = 1438 \text{ lb./ft.}$$

The wind load will be represented by a concentrated load P which will have the same moment about the base as a uniform pressure of 20 psf distributed over the frame height.

$$P = \frac{20 \text{ psf} \times 18 \text{ ft.} \times 17 \text{ ft.} \times 9 \text{ ft.} \times 1.41}{10 \text{ ft}} = 7770 \text{ lb.}$$

The side load parameter A is determined from the expression for P given in Fig. 1.

$$A = \frac{2Pa}{wL} = \frac{2 \times 7770 \text{ lb.} \times 0.25}{1438 \text{ lb./ft.} \times 40 \text{ ft.}} = 0.0675$$

Fig. 6 shows that the frame will form a composite mechanism under either loading. M_p as given by Eq. (2) or the appropriate curve from Ref. 6 will be:

$$M_p = 0.0456\ wL^2$$

when A = 0 and

$$M_p = 0.0532\ wL^2$$

when A = 0.0675

The section modulus required without wind is

$$Z = \frac{M_p}{\sigma_y} = \frac{0.0456 \times 1.918\ k/ft. \times 40\ ft. \times 12 \times 40\ in.}{33\ ksi}$$

$$= 50.8\ in^3$$

The section modulus required with wind is:

$$Z = \frac{0.0532 \times 1.438\ k/ft \times 40\ ft \times 12 \times 40\ in.}{33\ ksi}$$

$$= 45.6\ in^3$$

The case without wind controls.

Section economy tables will give a 14 WF 34 with $Z = 54.5\ in^3$. However, in the event delivery on 14 WF 34 could not be obtained, or for some reason it was desired to use a shallower member, a 12 WF 36 with $Z = 51.4\ in^3$ would suffice. The 12 WF 36 member will be selected for this example.

b. Hinge Angle and Deflections

The hinge angles and deflections for this frame are given in Figs. 10, 13, 14, and 15. Entering the charts with b = 0.2, a = 0.25, and A = 0, the following values are obtained:

From Fig. 10

$$H_E = 0.62\ \phi_p L$$

From Fig. 13

$$\delta_E = 0.117\ \phi_p L^2$$

From Fig. 14

$$\delta_C = 0.036\ \phi_p L^2$$

From Fig. 15

$$\delta_D = 0.1005\ \phi_p L^2$$

By substituting the known values for ϕ_p and L, these functions may be evaluated as follows:

$$\phi_p L = \frac{MpL}{EI} = \frac{33 \text{ ksi} \times 51.4 \text{ in.}^3 \times 480 \text{ in.}}{30 \times 10^3 \text{ ksi} \times 280.8 \text{ in}^4}$$

$$= 0.0966 \text{ rad.}$$

$$\phi_p L^2 = 46.4 \text{ in.}$$

$$H_E = 0.62\ \phi_p L = 0.060 \text{ rad.}$$

$$\delta_E = 0.117\ \phi_p L^2 = 5.43 \text{ in.}$$

$$\delta_C = 0.036\ \phi_p L^2 = 1.67 \text{ in.}$$

$$\delta_D = 0.1005\ \phi_p L^2 = 4.66 \text{ in.}$$

...(33)

c. Comparison with Experimental Results

Test results are available for a 40 ft. span gabled frame with 12 WF 36 members.[4] This frame was loaded with four vertical concentrated loads and had fixed bases and a slightly different roof slope, but was similar enough to allow the hinge angles to be compared. The moment diagrams for the two frames are plotted in Fig. 16 showing this similarity. The lee knee of the test frame rotated through a measured angle of 0.077 radians at the end of the test with the frame

still at maximum load as compared with the 0.060 radian requirement for the theoretical frame. Of course a small part of this measured rotation was due to bending of the members in the length spanned by the rotation indicator and should not be included in the comparison of hinge angles. This amount was calculated as approximately 0.005 radians. This result indicates that the theoretical frame would probably be satisfactory just as the test frame was.

The vertical deflection of the test frame just as it reached maximum load was 5.3 inches as compared with 4.57 inches required for the theoretical frame. However, the test frame was able to sustain the maximum load through a total deflection of 9.9 inches.

Due to the fixity of the bases and the smaller roof slope of the test frame, it is not surprising that the total horizontal deflections of the knees were less than those theoretically required for the pinned-base frame. The experimental deflections were 3.9 in. for the lee knee and 1.6 for the windward knee as compared with 5.43 and 1.67 respectively, for the theoretical pinned-base frame.

4. PROBABLE EXTREME VALUES OF HINGE ANGLES

4.1 EXTREME VALUES OF LOADING AND GEOMETRY

Since one of the primary objectives of this study is to determine extreme values of the hinge angles, some attention will be given to the extreme ranges of the factors controlling hinge angles. In the proceeding sections it has been shown that a frame may be designed and the magnitude of the required angle determined if the following factors are known:

(1) Span length, L.

(2) Bent spacing, s

(3) Column height, aL

(4) Roof rise, bL

(5) Vertical load intensity, w.

(6) Horizontal concentrated load, P = AwL/2a

The first four factors are geometric factors which are generally controlled by architectural considerations. The last two factors are the load factors which are determined by the design allowances made to take care of dead load, live load, and wind load. An estimate of the probable range of each of these variables in typical rigid frame designs was made on the basis of various structural and architectural discussions in available literature.[5,7, 8, 9, 10, 11] From this estimate, the range of variables to be studies was limited to the values given in Table I. A detailed description of how each of the values in Table I was selected is given in Ref. 2.

TABLE I

Extreme Values of Geometry and Loading

	Column Height Factor a	Roof Rise Factor b	b/a	Bent Spacing s	Horizontal Wind Pressure p	Vertical Unit Load q
Minimum	0.167	0	0	L/8	0/20 psf	60 psf
Maximum	1.0	0.5	1.0	L/2	70 psf	60 psf

In calculating the hinge angles required for a frame, the value of the side load factor, A, is required as well as the dimensions of the structure. The side load factor, A, is defined as the quantity 2 Pa/wL. P is the horizontal concentrated load at the eaves which will give the same overturning moment about the base as a uniformly distributed wind load on the vertical projection of the frame. From the quantity 2 Pa/wL, it can be seen that A depends on the vertical load and horizontal wind pressure combined with the dimensions of the structure. By making different combinations over the range of variation of these independent variables, Table II was prepared giving the maximum value of side load factor, A, consistent with several geometries of structure and two ranges of wind pressure. Realizing that A = 0 for no wind load, it is seen in Table II that for the typical 20 psf wind load, the side load factors may range from 0 to 0.333 for flat roofed frames and from 0 to 0.750 for gabled frames. Thus the possibilities of actual loads cover the whole range of A values for which hinge angles have been calculated and charted. For the extreme case of

a 70 psf wind load, "A"-values less than 1.0 will include all structures except those with the largest column heights. For the cases with long columns, it is probable that the hinge angles will be smaller than the values plotted for A = 1 and at least an upper bound for the hinge angles is included in the curves. (Fig. 10).

TABLE II

Maximum Values of Side Load Factor A

Wind Load	Column Height Factor a	Roof Rise Factor b	Maximum Side Load Factor A
Flat Roofed Frames			
20 psf	0.2	0	0.01333
	0.5	0	0.0833
	1.0	0	0.333
70 psf	0.2	0	0.0467
	0.5	0	0.292
	1.0	0	1.166
Gabled Frames			
20 psf	0.2	0.2	0.0533
	0.5	0.5	0.333
	1.0	0.2	0.480
	1.0	0.5	0.750
70 psf	0.2	0.2	0.1867
	0.5	0.5	1.167
	1.0	0.2	1.680
	1.0	0.5	2.62

4.2 EXTREME VALUES OF HINGE ANGLES

The maximum probable hinge angles for several extremes of size and loading were calculated and are shown in Table III along with a list of the factors causing the extreme values of each.

The maximum probable values of hinge angles can either depend on the maximum angle shown on Figs. 9 or 10 or on the maximum angle possible within the limits of the probable side load factors, A, given in Table II.* For example, in flat roofed frames with 20 psf wind loading, the maximum hinge angle at the lee knee with long columns would be about 0.32 $\emptyset_p L$ with A = 0.333. At the same time the maximum for short columns would be about 0.22 $\emptyset_p L$ with A limited to 0.01333 even though, for a= 0.2, greater values of the hinge are indicated for values of A up to 0.5. Another limit for flat-roofed frames would be a hinge angle, H_F, in the beam of 0.33 $\emptyset_p L$ for no side load and a column height equal to the span.

If a 70 psf wind is specified on a flat-roofed frame, the same maximum value of $H_F = 0.33\ \emptyset_p L$ would apply (with no side load and a = 1.0). The hinge angle, H_E, at the lee knee could increase to 0.42 $\emptyset_p L$.

Applying the same type of reasoning to gabled frames shows that the intensity of the wind pressure has little effect on the maximum values of the hinge angles H_E and H_F. H_E has its maximum value for very short columns and relatively light side loads; thus, the

---

* Hinge angles for frames with b = 0.5 were calculated, but the curves are not included in this report. However, the results are used in this discussion.

greater sideloads actually mean a decrease in required hinge angle. The hinge angle H_F in the rafter has its maximum value with no side load and with the longest columns and flattest roofs. One additional factor is introduced in gabled frames - this is the possibility of a hinge angle H_C at the windward knee. The maximum angle occurs with a high wind load on a frame with short columns and a steep roof.

By picking the extreme values of hinge angles from Table III, it is seen that the maximum hinge angle at a lee knee would be about 1.03 $\phi_p L$ for a steep gabled frame. (b = 0.5, a = 0.5, A = 0.1). The maximum hinge angle for a windward knee would also occur in a steep gabled frame, (b = 0.5, a = 0.5, A = 1.17) with a value of about 0.49 $\phi_p L$. The maximum hinge angle in the rafter would occur with a flat roofed frame and would be 0.33 $\phi_p L$. (b = 0, a = 1.0, A = 0).

TABLE III

Maximum Probable Hinge Angles for Single Span Frames

	Hinge Angle at Lee Knee H_E	Hinge Angle At Windward Knee H_C	Hinge Angle In Windward Rafter H_F
Factors Causing Maximum Hinge Angle	Small Side Load Short Columns Steep Roofs	High Side Load Short Columns Steep Roofs	No Side Load Tall Columns Low Roofs
<u>Wind Load</u> Flat Roofed Frames b = 0 Up to 20 psf Up to 20 psf	 0.32 $\emptyset_p L$ 0.42 $\emptyset_p L$	 ——— ———	 0.33 $\emptyset_p L$ 0.33 $\emptyset_p L$
Gabled Frames b = 0.2 Up to 20 psf Up to 70 psf b = 0.5 Up to 20 psf Up to 70 psf	 0.80 $\emptyset_p L$ 0.86 $\emptyset_p L$ 1.03 $\emptyset_p L$ 1.03 $\emptyset_p L$	 ——— ——— ——— 0.44 $\emptyset_p L$	 0.15 $\emptyset_p L$ 0.15 $\emptyset_p L$ ——— ———

5. SUMMARY

The following summarizes the results of this study of rotation requirements for single-span gabled portal frames with pinned bases and including the special case of flat-roofed frames.

(1) Equations were developed determining the domains of two types of mechanisms (Eq.(3), Fig. 3).

(2) Equations were developed determining the domains in which any of three possible plastic hinges could be the first to form (Eq. (8), (9) and (10), Fig. 4).

(3) Combining the graphs for type of mechanism and location of the first plastic hinge gives graphs indicating four combinations of mechanism and first plastic hinge (Fig. 6).

(4) Expressions and charts, were developed for the hinge angles, H, for the four cases of failure mode (Figs. 10 and 11).

(5) Equations and charts were developed for the horizontal deflections of the columns and for the vertical deflections of the roofs (Figs. 11 through 15).

(6) A gabled frame was designed and the hinge angle requirements were calculated. These were compared with the actual hinge angles measured on a test specimen using the same rolled structural sections. Though the experimental loading differed slightly from the theoretical loading, they were considered similar enough for a rough comparison (Fig. 6). The comparison showed the theoretical and experimental hinge

angles to be of the same order of magnitude.

(7) The maximum possible hinge angles were determined for a complete range of frame proportions and for wind loadings ranging from zero to 70 psf, including the usually specified wind load of 20 psf. These calculations showed the maximum hinge angle at a lee knee to be about $1.03\ \phi_p L$ for gabled frames with small side loads, short columns and steep roofs. The maximum hinge angle at a windward knee would be about $0.44\ \phi_p L$ for gabled frames with large side loads, short columns, and steep roofs. The maximum hinge angle in a beam or rafter would be about $0.33\ \phi_p L$ for flat-roofed frames with tall columns and no side load.

The method of solution used in this report has also been adapted to the solution of rotation requirement problems for multi-span frames. Later reports will present the solutions for flat-roofed and gabled multi-span frames with pinned bases.

6. ACKNOWLEDGEMENTS

The author wishes to express his appreciation for the helpful suggestions and criticisms made by several of the research personnel at Fritz Engineering Laboratory during the development and preparation of the work presented in this paper. Dr. Robert L. Ketter was especially helpful in lending the full use of his calculations on the plastic design of frames. Le Wu Lu checked the theoretical derivations and carried out many of the numerical calculations for the resulting curves.

The analytical work described in this report is part of a project on "Welded Continuous Frames and Their Components" being carried out under the direction of Lynn S. Beedle. The project is sponsored jointly by the Welding Research Council and the U. S. Navy Department under an agreement with the Institute of Research of Lehigh University. Funds are supplied by the American Institute of Steel Construction, American Iron and Steel Institute, Office of Naval Research, Bureau of Ships, and the Bureau of Yards and Docks. The work was done at Fritz Engineering Laboratory of which Professor William J. Eney is Director.

7. NOMENCLATURE

Symbols:

A	non-dimensional parameter relating the horizontal force acting on a structure (or the "overturning" moment of one part of a structure on the adjacent part) to the vertical loading. It is assumed that "A" results in positive work being done as the structure fails.
E	Young's modulus of elasticity
F	load factor of safety
F	dimensionless parameter in elastic moment equation
G	dimensionless parameter in elastic moment equation
H	hinge angle
I	moment of inertia of cross section
J	dimensionless parameter in elastic moment equations
L	span length
M	moment
M_{FN}	moment at far end of member
M_{NF}	moment at near end of member
M_p	plastic hinge moment
N	dimensionless parameter in elastic moment equations
P	concentrated horizontal load
R	rotation of a chord between ends of a member
Z	fully plastic section modulus
a	ratio of column height to frame span
b	pitch, ratio of frame rise to span
ℓ	length of a member or portion of a member (variable)
p	horizontal wind pressure per unit area
q	uniformly distributed vertical roof load per unit area

s	bent spacing
w	uniformly distributed load per unit length of span
α	non-dimensional parameter defining the distance to the location of the plastic hinge in the rafter of a structure.
δ	deflection
θ	slope or rotation of a member from undeformed shape
σ_y	yield stress of steel
ϕ	curvature of member
ϕ_p	curvature parameter M_p / EI
Δ	displacement

Subscripts in Slope-Deflection Equations:

Single letter	--	joint
Double letter	--	member
First letter	--	near end
Second letter	--	far end

Important Functions for Frames:

δ_C	horizontal deflection of windward knee
δ_D	vertical deflection of ridge or center of flat roof
δ_E	horizontal deflection of lee knee
H_C	hinge angle in windward knee
H_D	hinge angle at ridge
H_E	hinge angle in lee knee
H_F	hinge angle in windward rafter

Definitions:

Plastic Hinge	A yielded section of a beam which acts as if it were hinged, except that it has a constant restraining moment.

Hinge Angle	The required rotation of a given plastic hinge in a structure that is necessary to assure that the structure reaches the ultimate load.
Rotation Capacity	The ability of a structural member to rotate at near-maximum moment.
Mechanism	A system of members (and/or segments of members) that can deform at constant load. It is used in the special sense that all hinges are plastic hinges (except pin ends).
Plastification of cross section	The development of full plastic yield of the cross section.
Redistribution of Moment	A process in which plastic hinges form successively in a redundant structure until the ultimate load of the structure is reached. In the process, a new distribution of moments is achieved in which portions of the structure which are less highly-stressed in the elastic state subsequently reach the plastic hinge value. Redistribution is accomplished by rotation through the hinge angle of earlier-formed plastic hinges.

8. REFERENCES

1. Beedle, L. S. Thurlimann, B. Ketter, R. L. — PLASTIC DESIGN IN STRUCTURAL STEEL 1955 Summer Course Lecture Notes, Lehigh University--AISC 1955.

2. Driscoll, G. C., Jr. — ROTATION CAPACITY REQUIREMENTS FOR BEAMS AND FRAMES OF STRUCTURAL STEEL, Ph.D. Dissertation, Lehigh University, 1958.

3. Driscoll, G. C., Jr. — ROTATION CAPACITY REQUIREMENTS FOR CONTINUOUS BEAMS, to be published in ASCE Proceedings.

4. Driscoll, G. C., Jr. — THE PLASTIC BEHAVIOR OF STRUCTURAL MEMBERS AND FRAMES, Progress Report No. 21, Welded Continuous Frames and Their Components, The Welding Journal, Research Suppl., June 1957, page 275-s

5. Griffiths, J. D. — SINGLE SPAN RIGID FRAMES IN STEEL, AISC, 1948.

6. Ketter, R. L. — PLASTIC DESIGN OF MULTI-SPAN RIGID FRAMES, Ph.D. Dissertation, Lehigh University, 1956.

7. Knudsen, K. E. Schutz, F. W. Beedle, L. S. — PROPOSAL FOR THE CONTINUATION OF PORTAL FRAME TESTS, Fritz Laboratory Report 205D.4 (Unpublished).

8. Korn, M. P. — A SHORT COURSE IN WELDED RIGID FRAME DESIGN, The Welding Journal, 36(3), p 236-239, March 1957.

9. Shedd, T. C. — STRUCTURAL DESIGN IN STEEL, John Wiley & Sons, Inc., 1934.

10. — STEEL CONSTRUCTION, American Institute of Steel Construction Handbook

11. — NATIONAL BUILDING CODE, National Board of Fire Underwriters, 1955, p 111, 272.

9. FIGURES

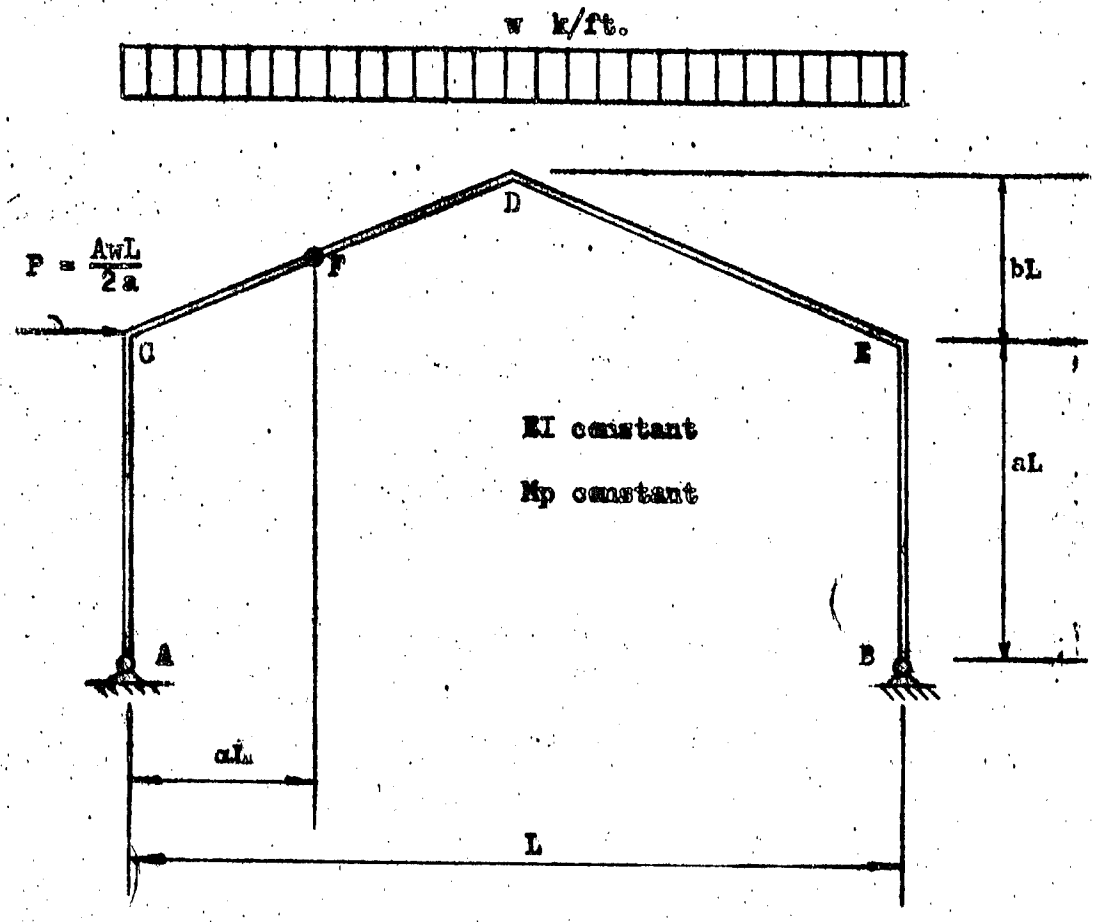

FIG. 4.1 FRAME DIMENSIONS AND LOADING

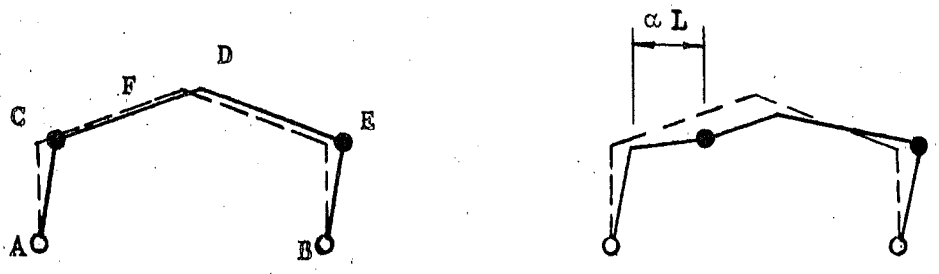

Panel Mechanism (a)

Composite Mechanism (b)

FIG. 2 POSSIBLE MECHANISMS FOR SINGLE-SPAN FRAME

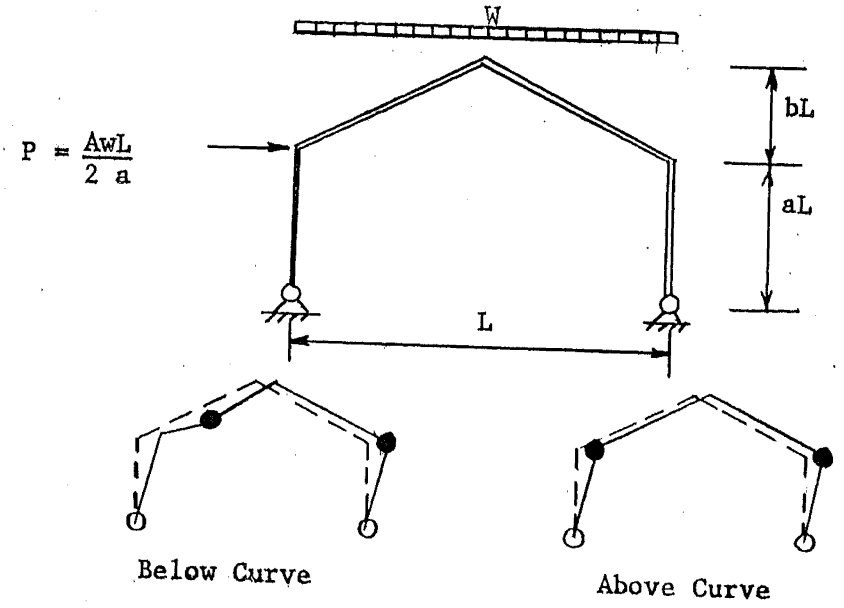

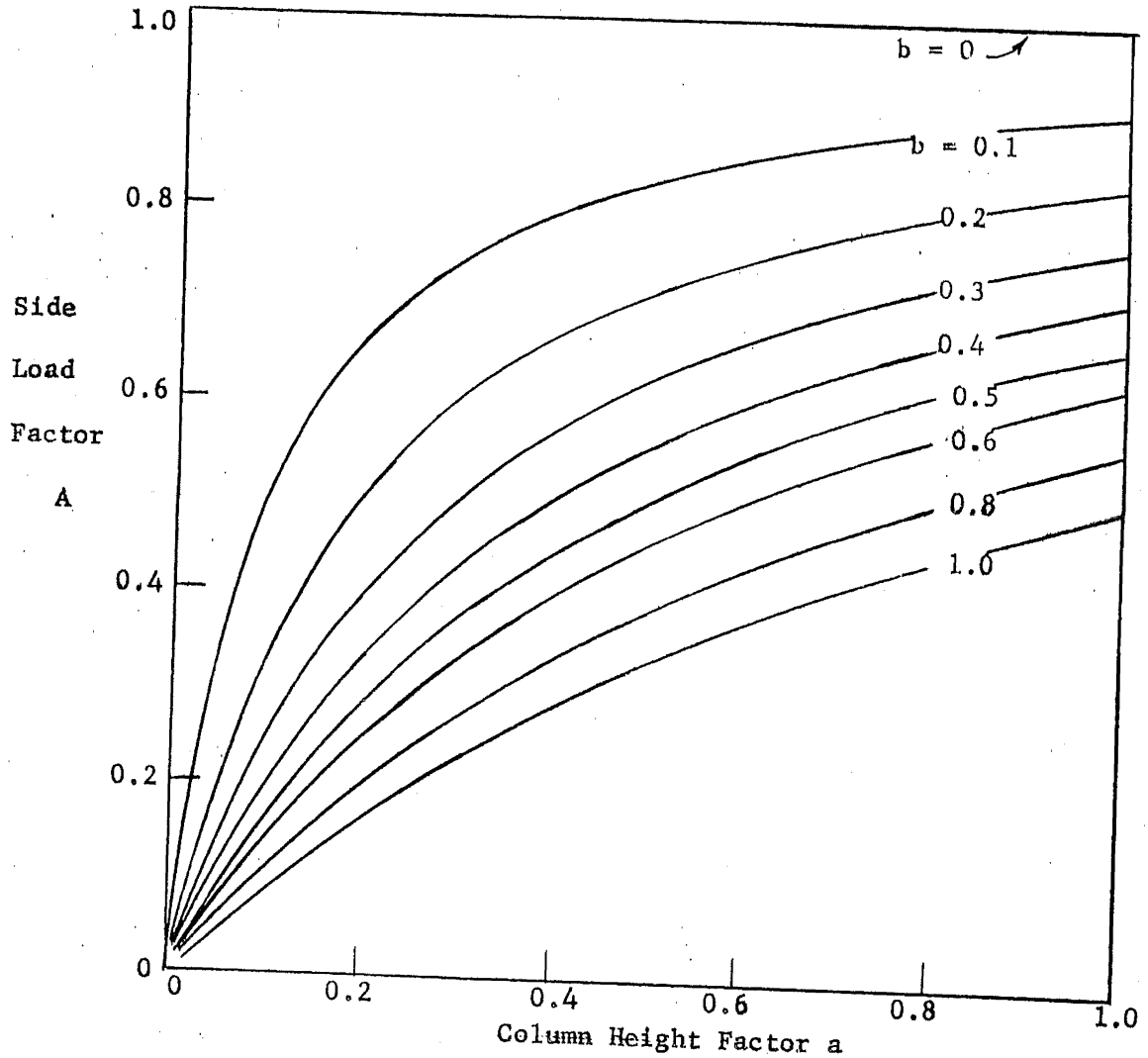

Fig. 3. TYPE OF MECHANISM

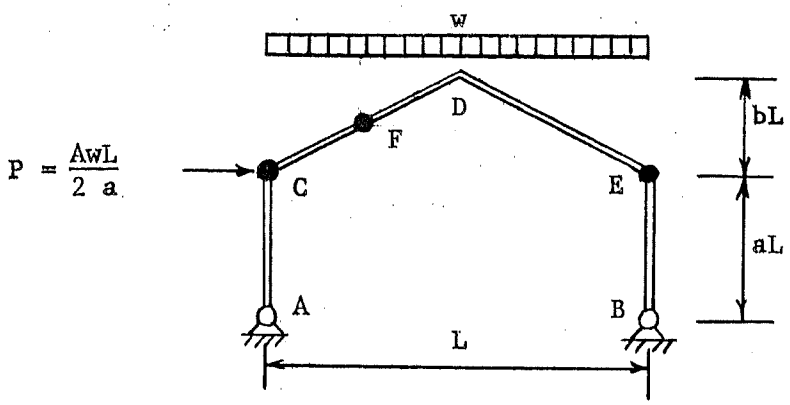

KEY:

Above Solid Line	-	First Hinge C
Below Dashed Line	-	" " F
Between Lines	-	" " E

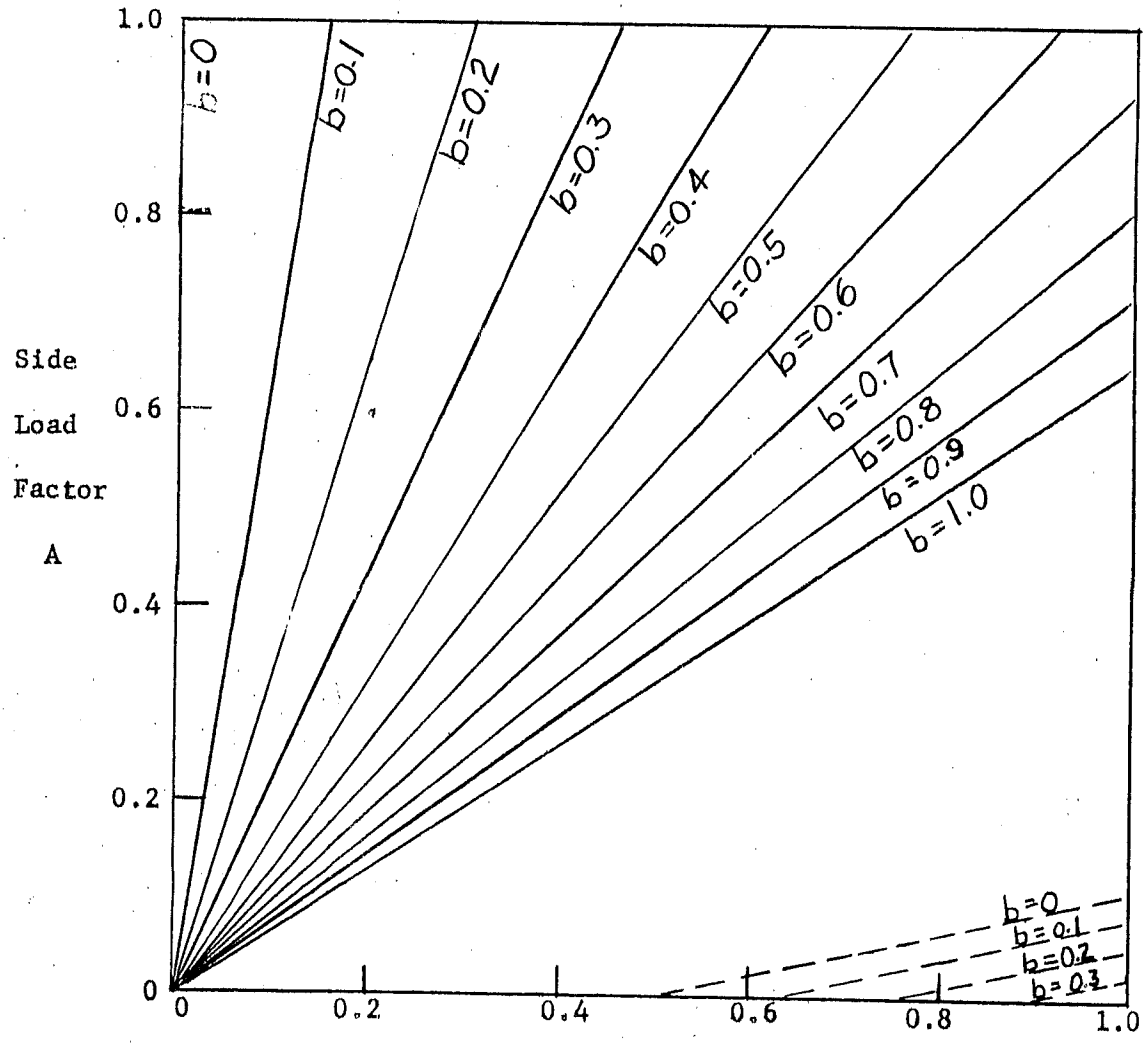

Fig. 4 LOCATION OF FIRST PLASTIC HINGE

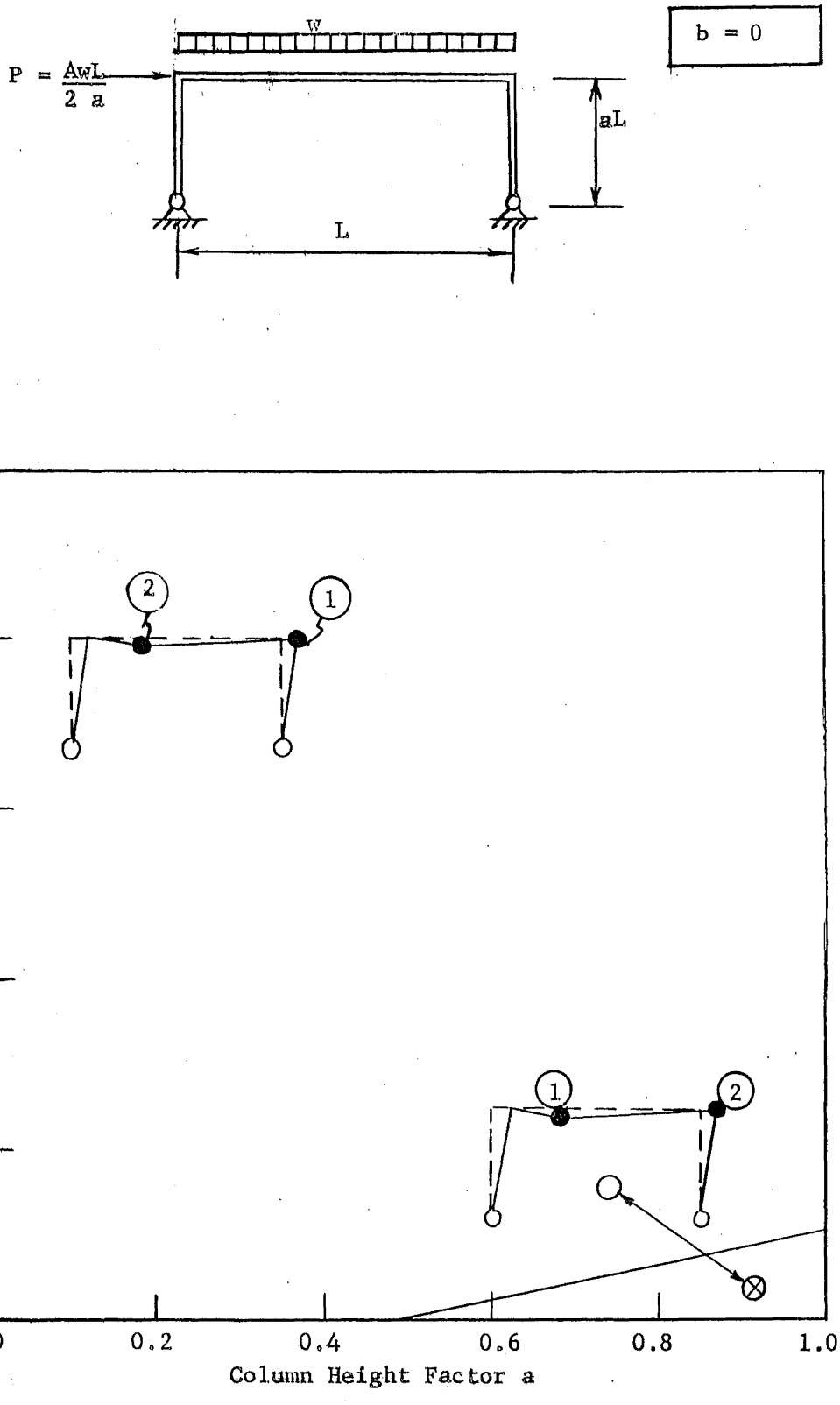

Fig. 5 LIMITS OF MECHANISMS (b = 0)

b = 0.2

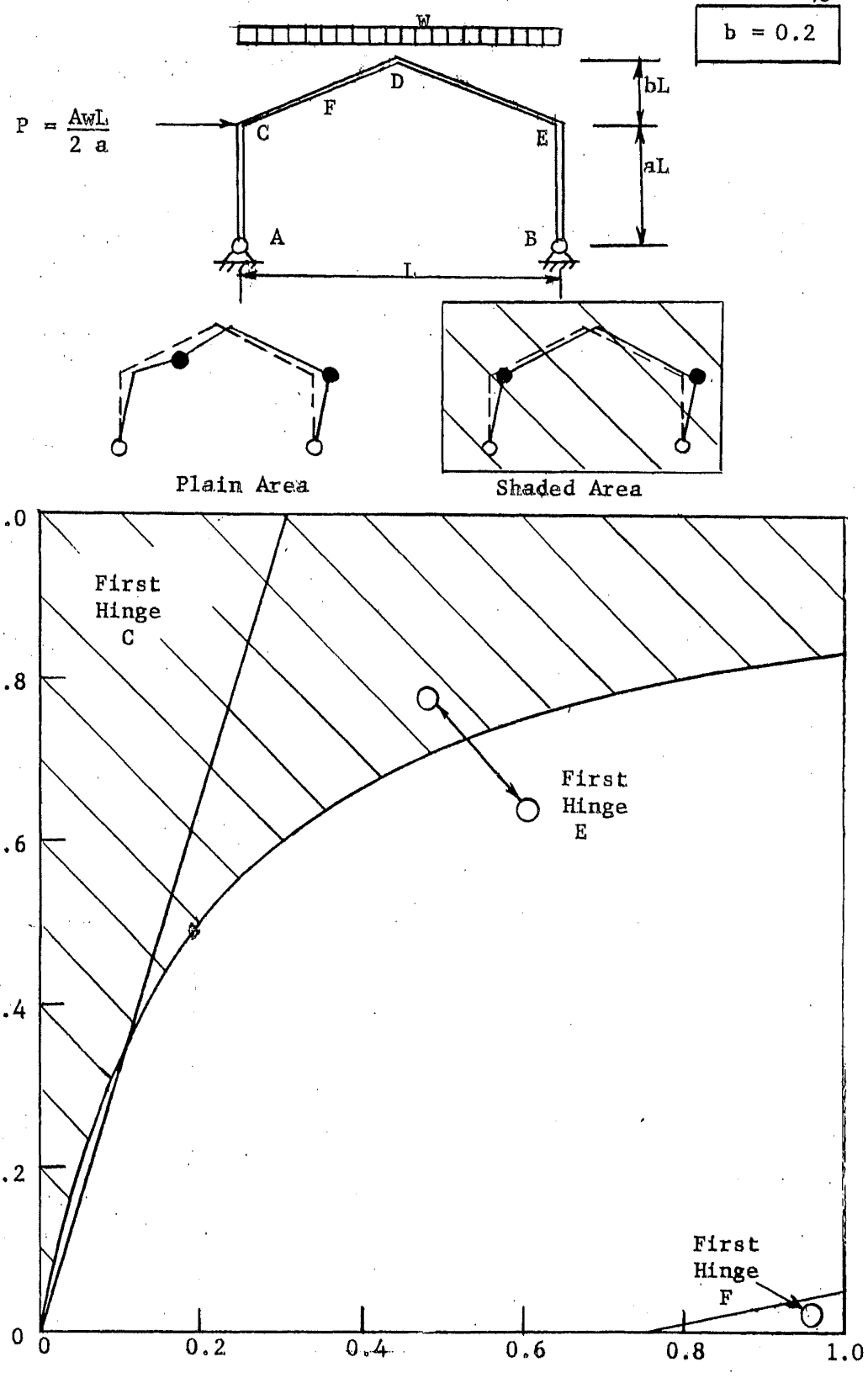

Fig. 6 LIMITS OF MECHANISMS (b = 0.2)

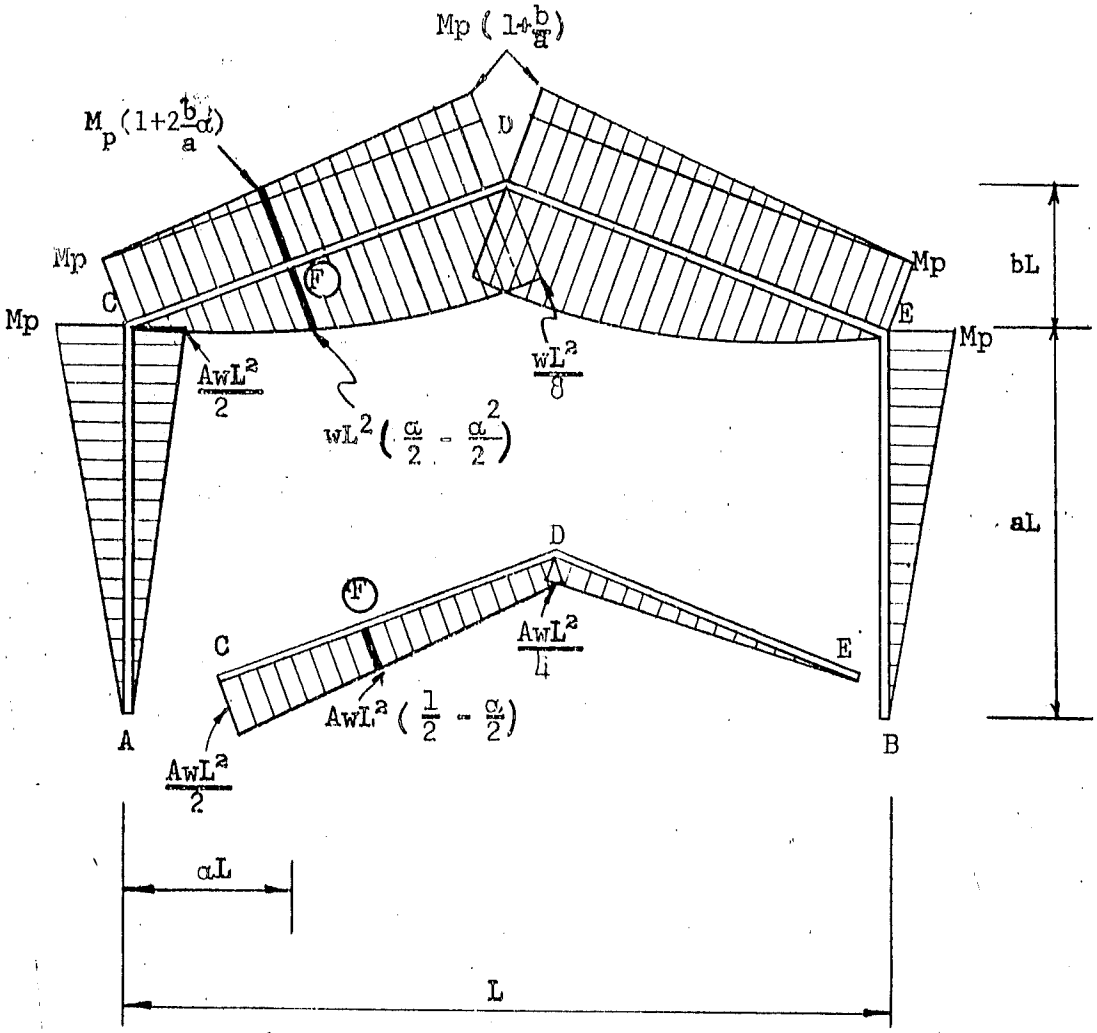

FIG. 5.8a. ULTIMATE LOAD MOMENT DIAGRAM

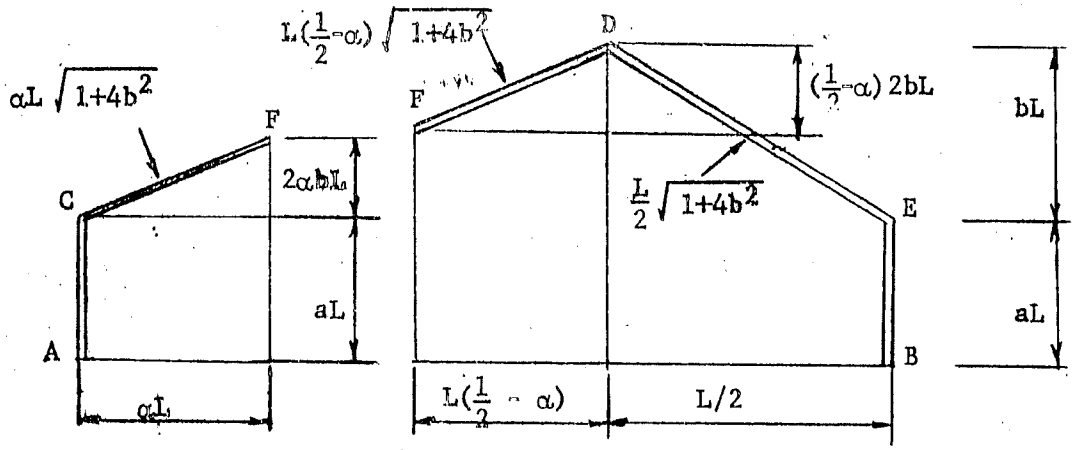

Fig. 5.8b. LENGTHS OF MEMBERS

$$\theta_{NF} = \theta'_{NF} + R_{NF} + \frac{\ell}{3EI} \left(M_{NF} - 1/2\ M_{FN} \right)$$

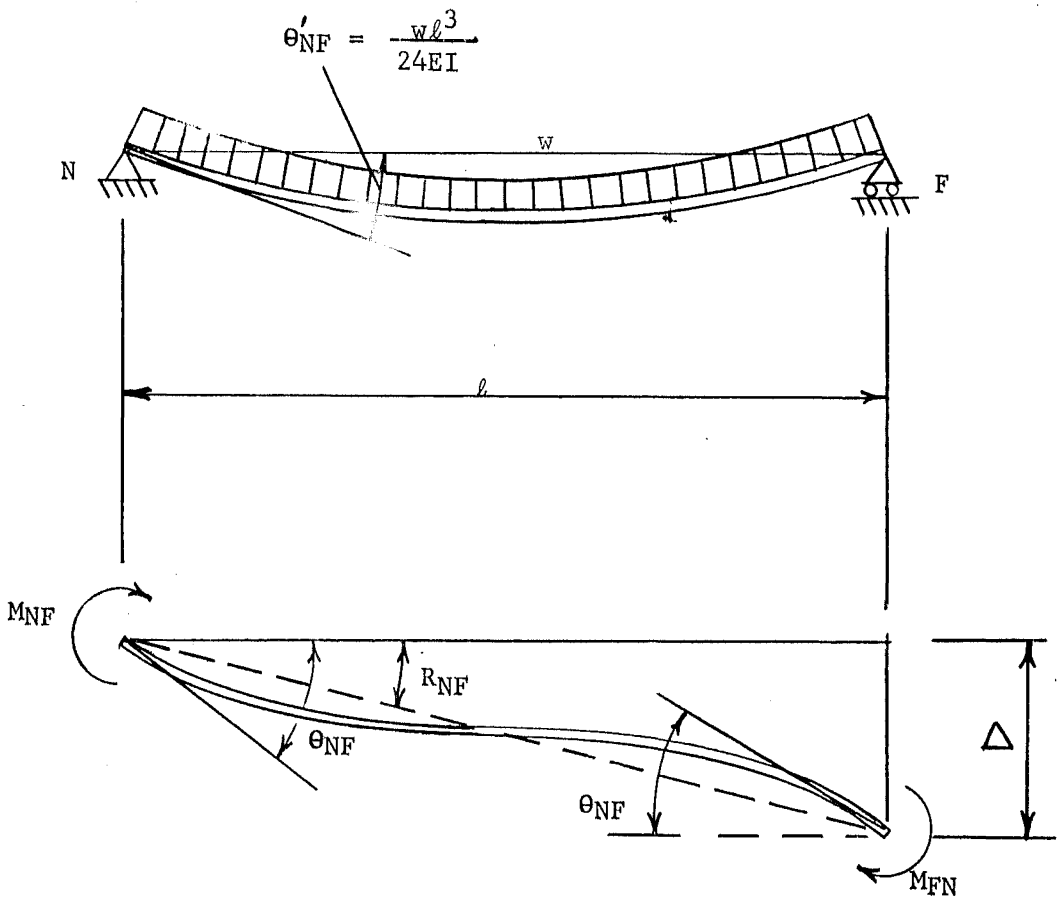

Fig. 8 Nomenclature for Slope-Deflection Equation

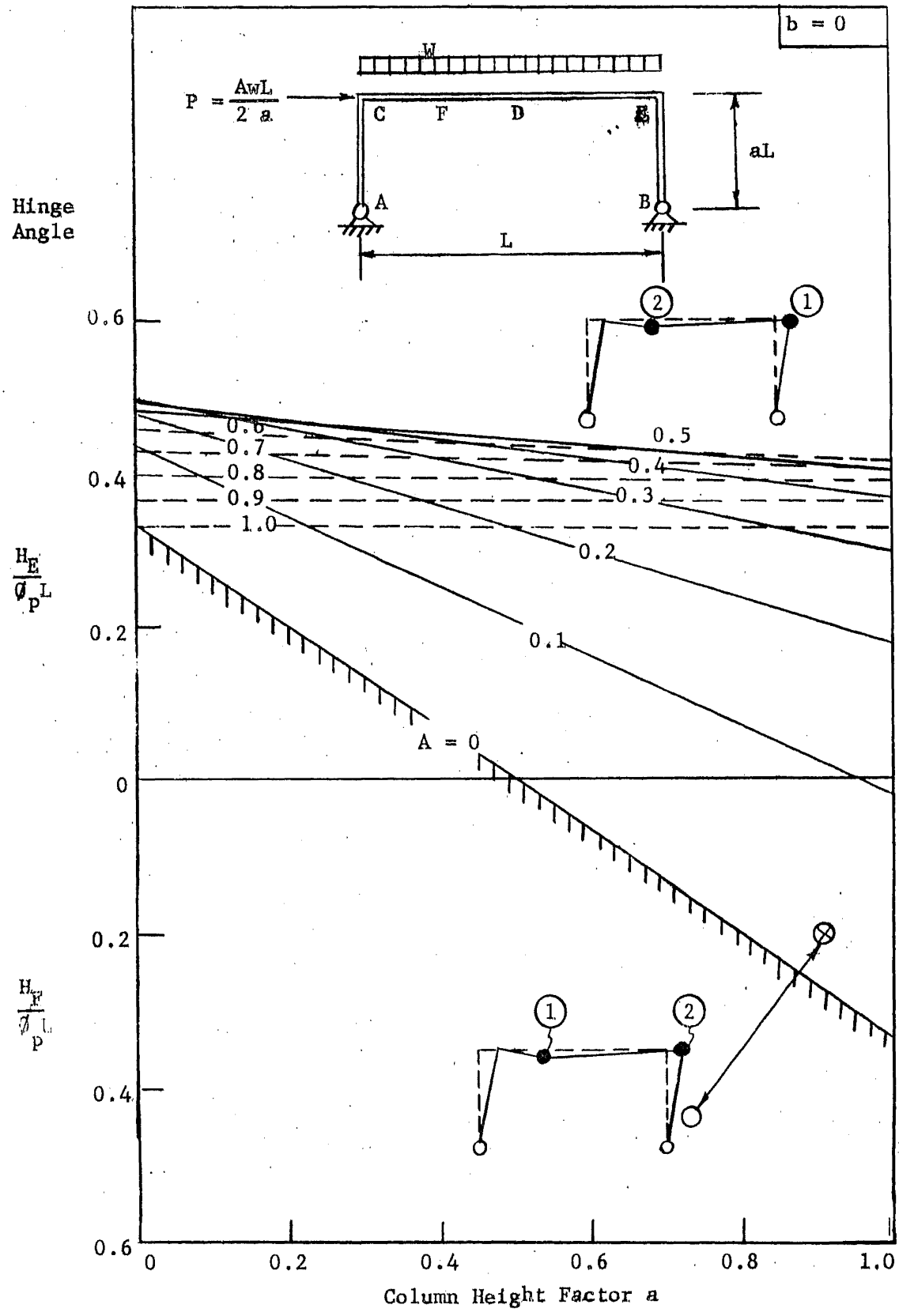

Fig. 9 HINGE ANGLES (b = 0)

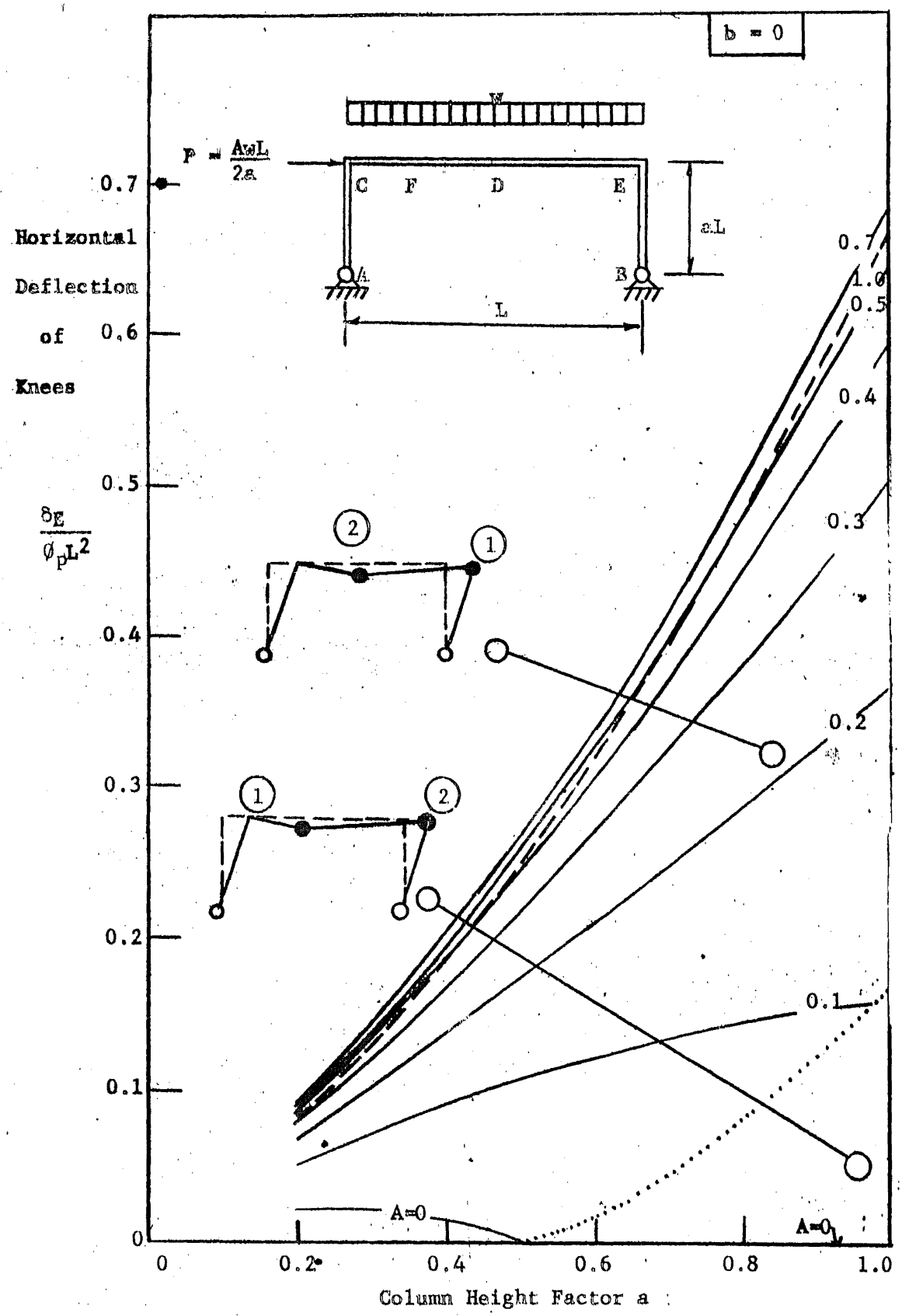

FIG. 11 HORIZONTAL DEFLECTION OF KNEES (b=0)

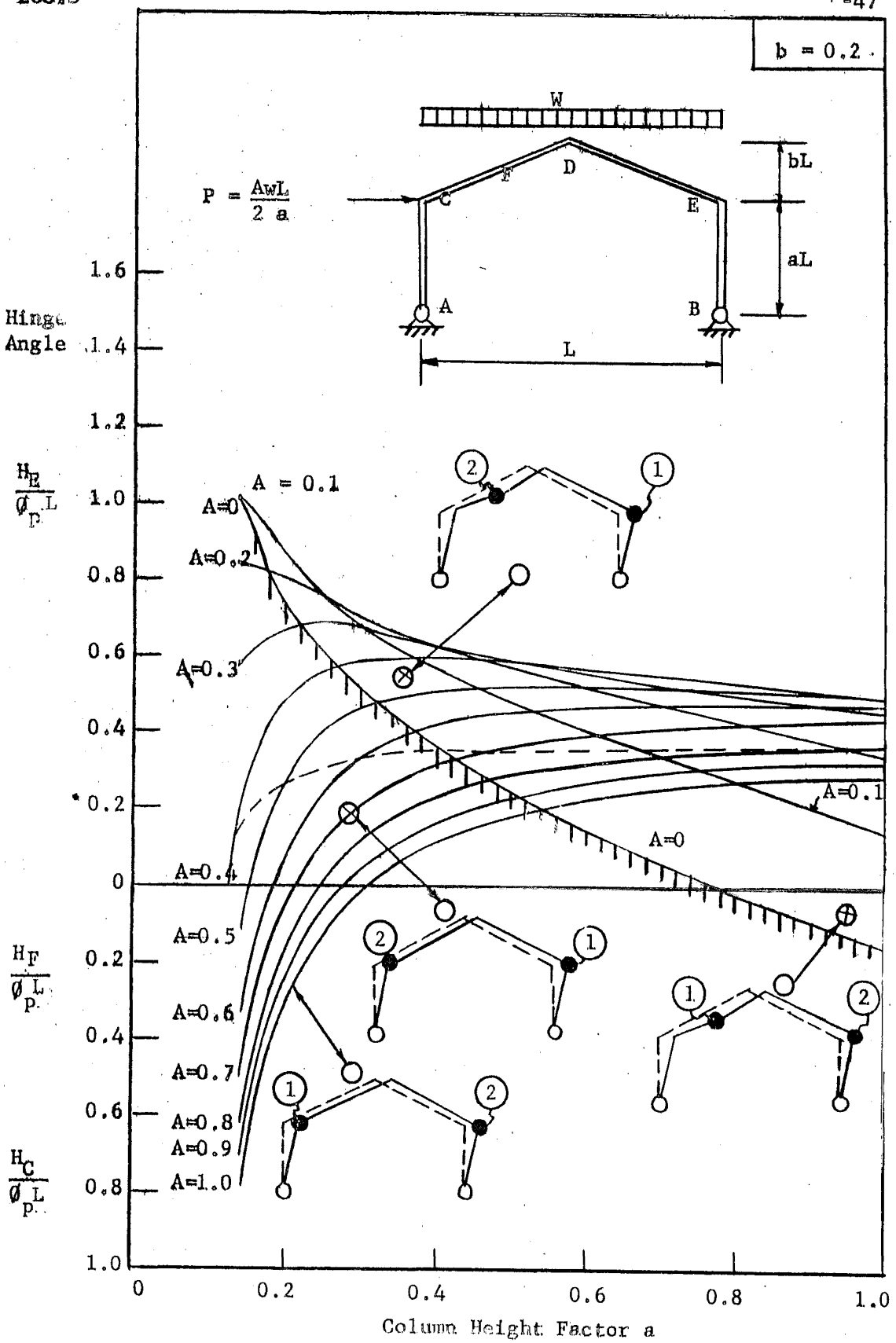

Fig. 10 HINGE ANGLES (b=0.2)

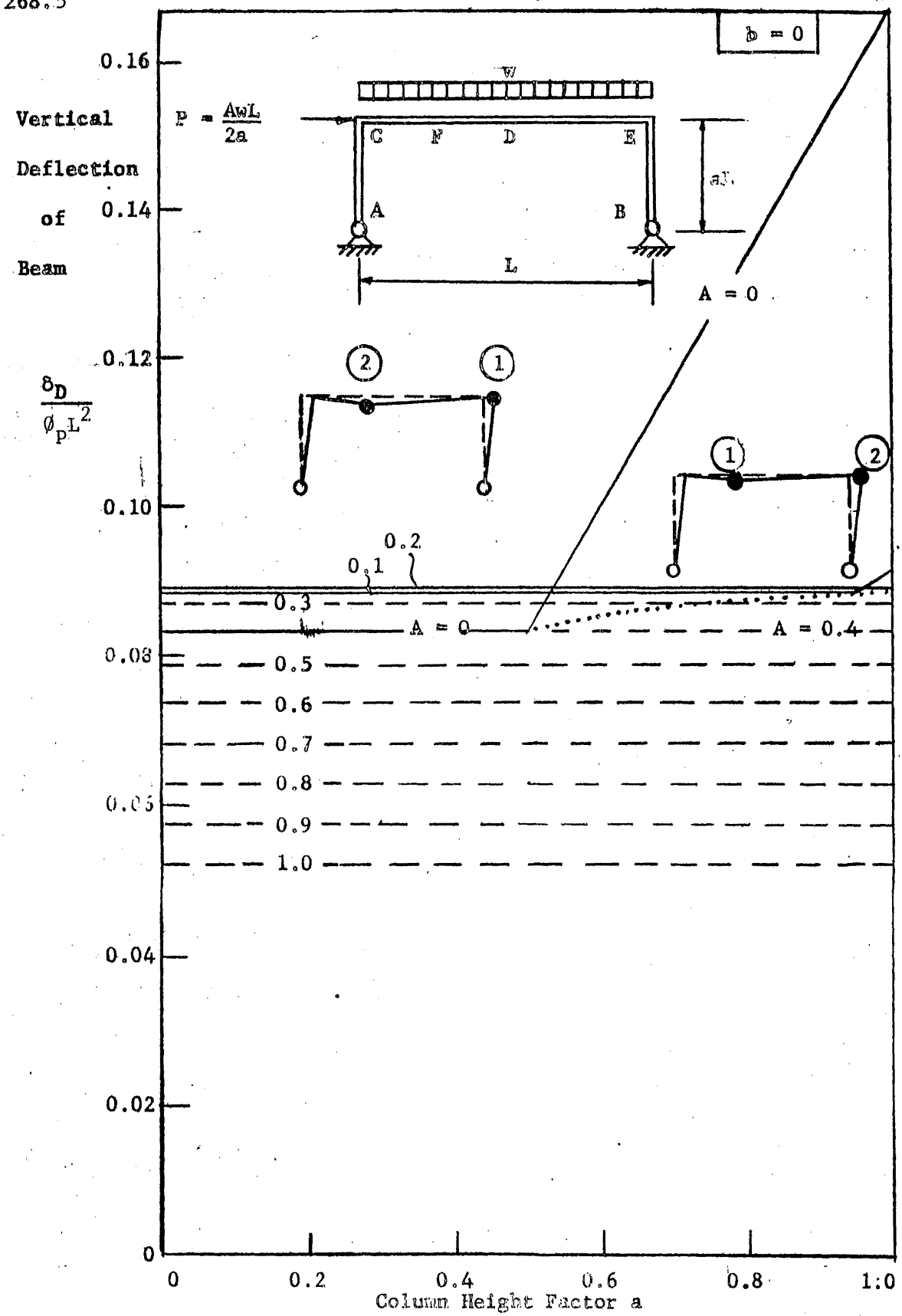

FIG. 12 VERTICAL DEFLECTION OF BEAM (b=0)

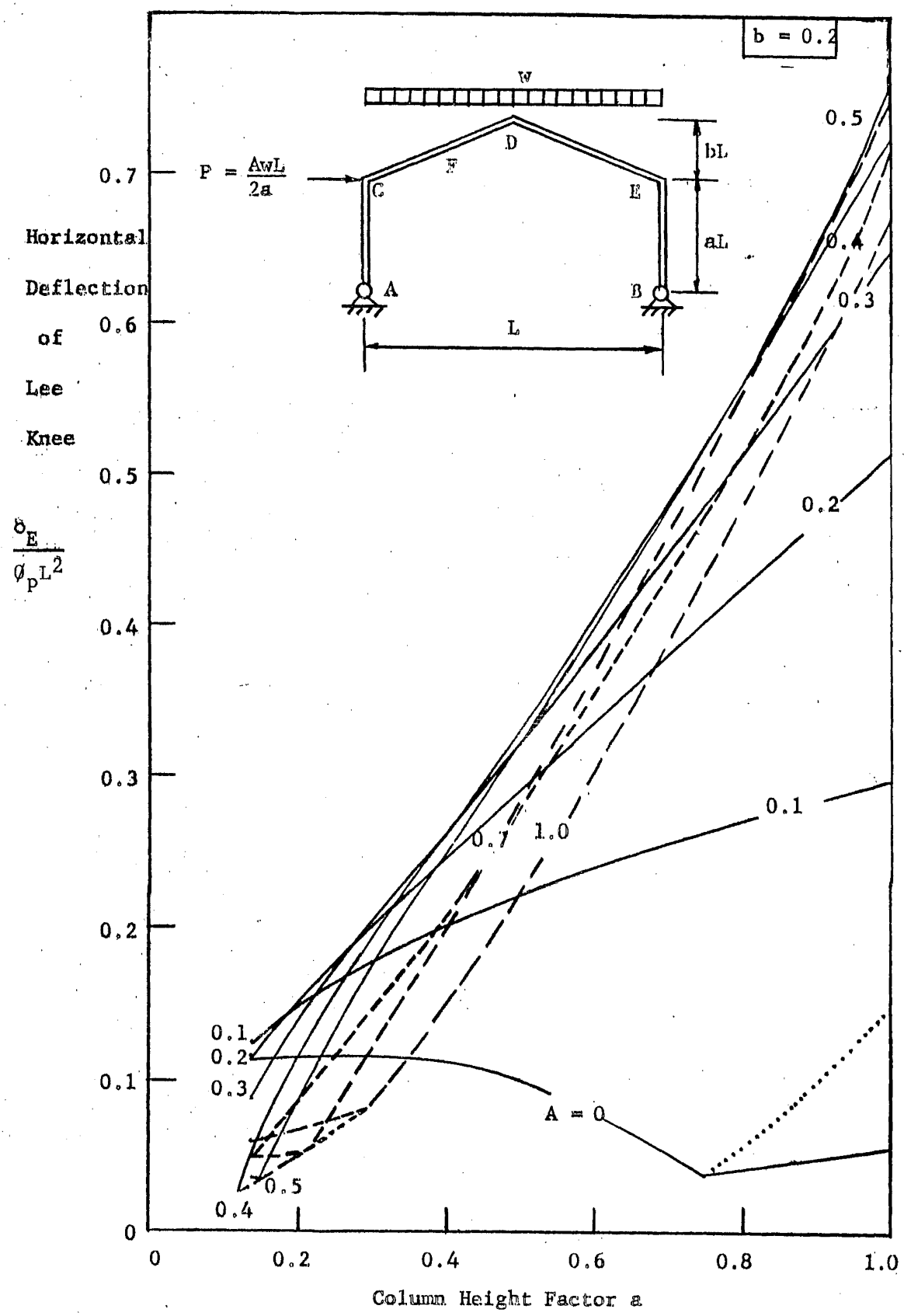

FIG. 13 HORIZONTAL DEFLECTION OF LEE KNEE (b=0.2)

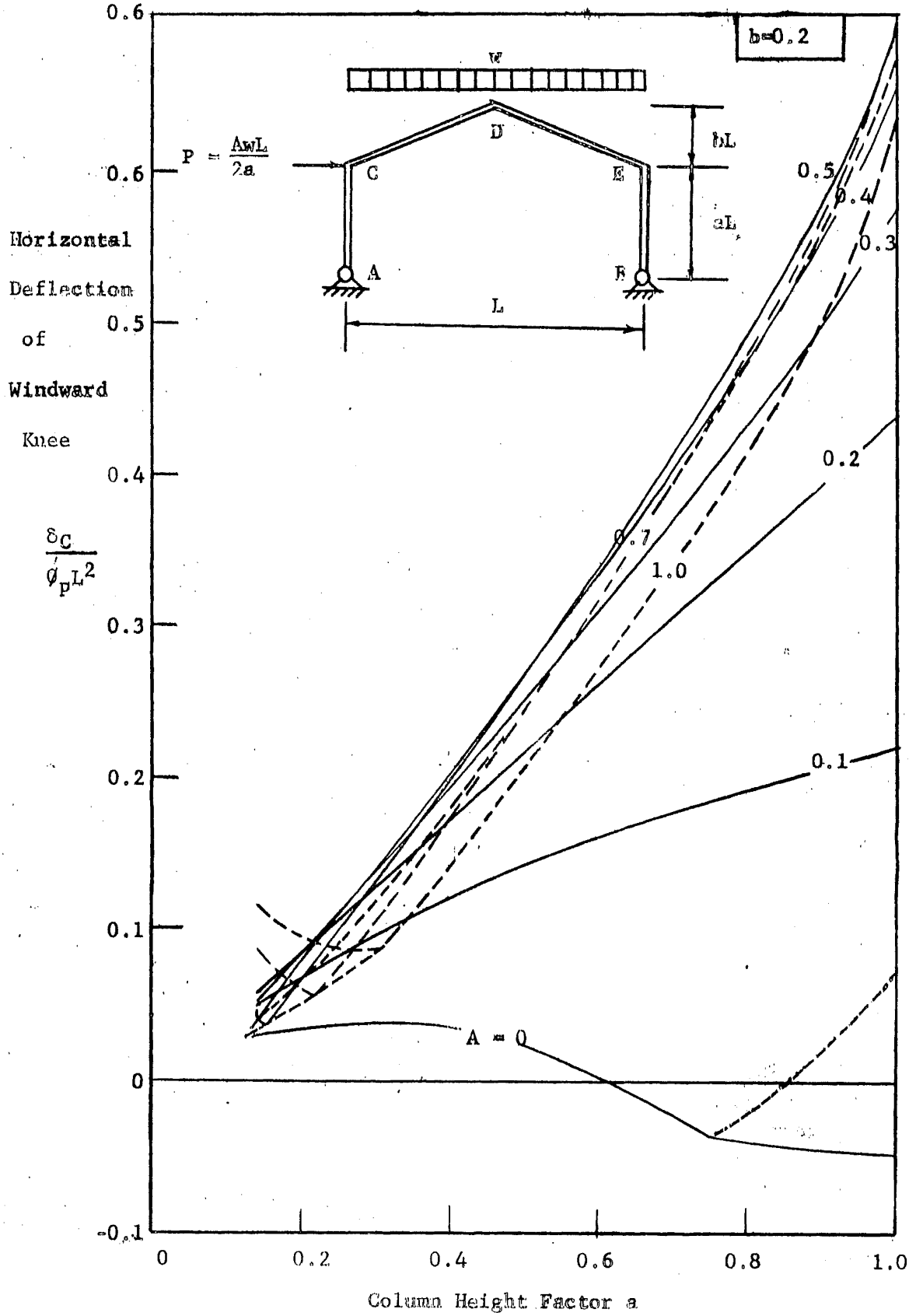

FIG. 14 HORIZONTAL DEFLECTION OF WINDWARD KNEE (b=0.2)

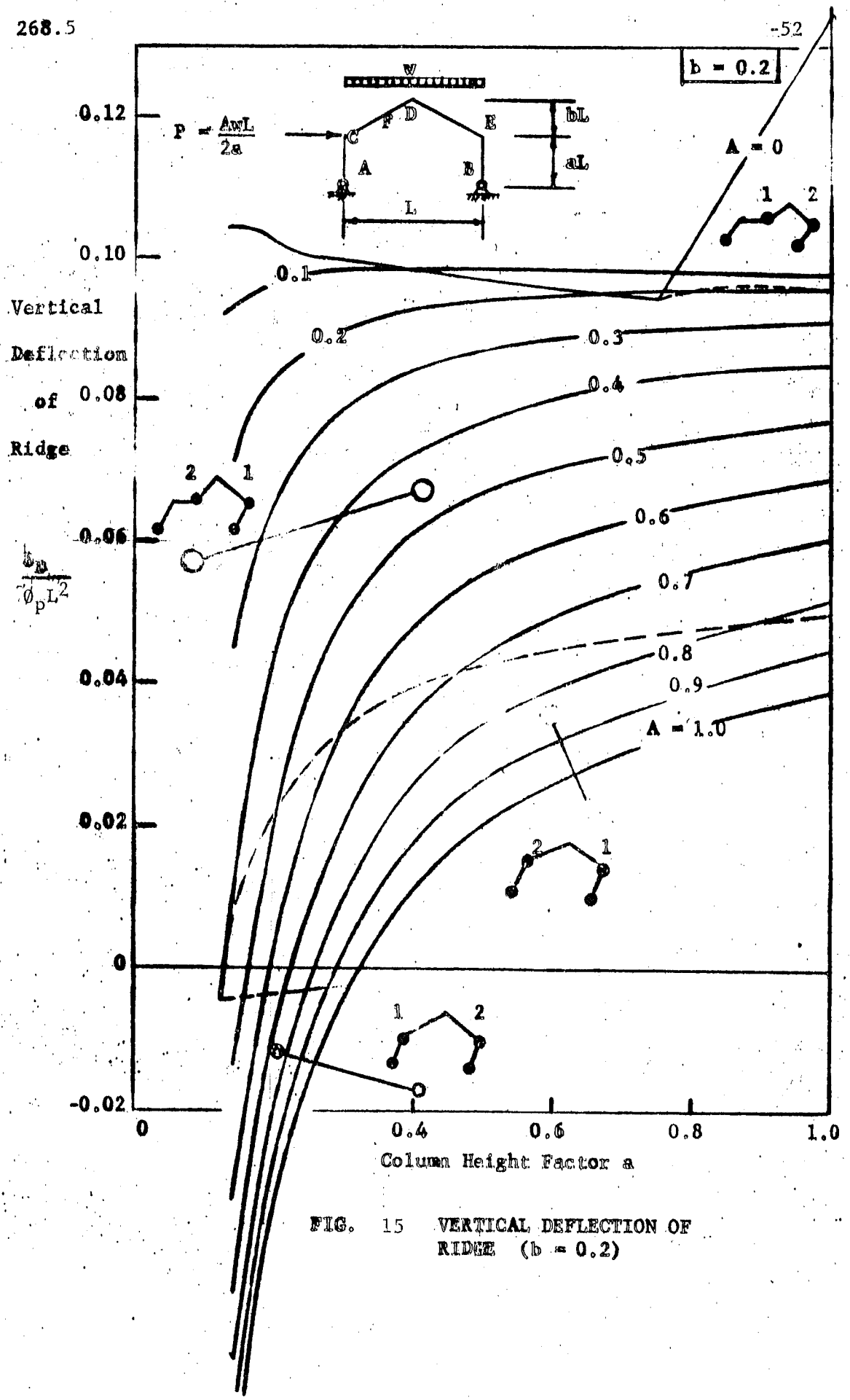

FIG. 15 VERTICAL DEFLECTION OF RIDGE (b = 0.2)

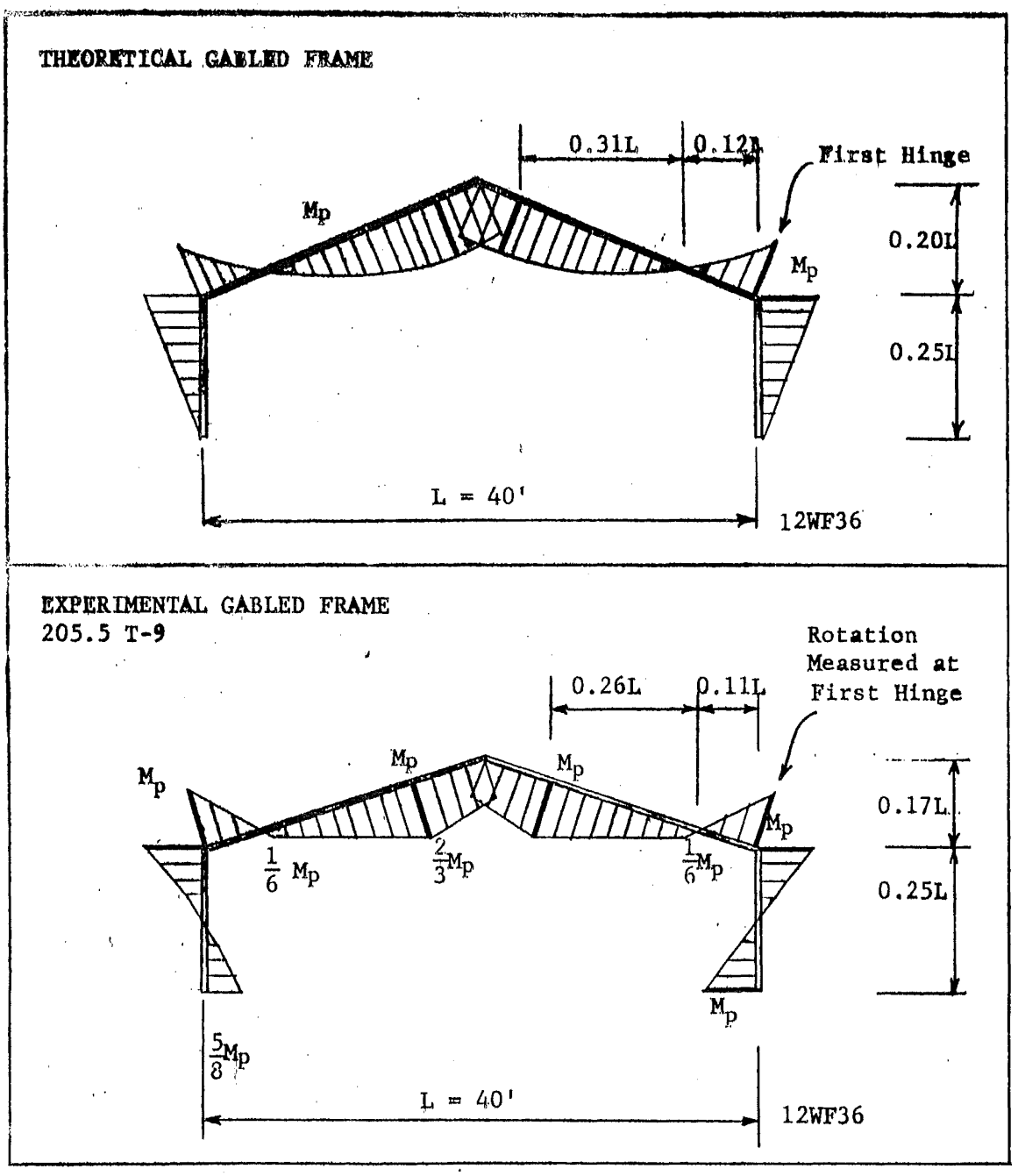

FIG 16 COMPARISON OF MOMENT DIAGRAM FOR THEORETICAL EXAMPLE OF GABLED FRAME WITH MOMENT DIAGRAM FOR EXPERIMENTAL TEST OF A GABLED FRAME